2021-05-01

Impact Of Various Hydrophobic Cargoes On The Structural Properties Of Pluronic-F127 Based Micelles Near The Standard Critical Transition Zone

Tahmida Raheen Iqbal
University of Texas at El Paso

IMPACT OF VARIOUS HYDROPHOBIC CARGOES ON THE STRUCTURAL PROPERTIES OF PLURONIC-F127 BASED MICELLES NEAR THE STANDARD CRITICAL TRANSITION ZONE

TAHMIDA RAHEEN IQBAL

Master's Program in Physics

APPROVED:

Jose Leobardo Bañuelos, Ph.D., Chair

Marian Manciu, Ph.D.

Ahmed A El-Gendy, Ph.D.

Mahesh Narayan, Ph.D.

Stephen L. Crites, Jr., Ph.D.
Dean of the Graduate School

Dedication

I dedicate this thesis to my family and friends along with all hard working and respected teachers for showering affection, love, and encouragement.

IMPACT OF VARIOUS HYDROPHOBIC CARGOES ON THE STRUCTURAL PROPERTIES OF PLURONIC-F127 BASED MICELLES NEAR THE STANDARD CRITICAL TRANSITION ZONE

by

TAHMIDA RAHEEN IQBAL, M.S.

THESIS

Presented to the Faculty of the Graduate School of

The University of Texas at El Paso

in Partial Fulfillment

of the Requirements

for the Degree of

MASTER OF SCIENCE

Department of Physics

THE UNIVERSITY OF TEXAS AT EL PASO

May 2021

ACKNOWLEDGEMENT

Research is more about teamwork than individual work. My research work would not have been completed without remarkable support from my research advisor Dr Jose L. Bañuelos. His constant guidance, patience, motivation, and immense knowledge is the force behind the success of my research work. I could not have imagined having a better mentor for my MS research and Dr Bañuelos is the best professor I have ever had in my academic career.

I would like to thank all members of "Nanomaterials, Interfaces, and Confinement for Energy and the Environment ($NICE^2$) Lab", especially Omar Avina, Ramon Ogaz and Kyle Williams, for helping me to conduct the research.

I would like to thank Dr Rajendra Zope, Dr Ahmed El-Gendy and Dr Mark R Pederson for enlightening lectures, proper guidance and support that ultimately paved the way for my research.

Finally, I must record a debt to my father Kazi Salahuddin Iqbal, mother Zameela Sultana, sister Mishkat Asfia Ikram, brother Kazi Arif Mahmud Iqbal and husband Kazi Tasnif Islam for their constant inspiration, love and support, that ultimately resulted in the birth of my master's thesis.

ABSTRACT

Pluronic F-127 is a triblock copolymer (PEO-PPO-PEO) that can form a micelle at critical micelle concentration (CMC). CMC for Pluronic F-127 is 0.7% at 25 ^{0}C. Micelles are lipid molecules that can arrange themselves in a spherical form in an aqueous solution with a hydrophobic core and hydrophilic shell. Pluronic F-127 can encapsulate poor water-soluble drugs and administrate the medicine to the targeted area with a controlled drug release rate and low toxicity. The purpose of this study is to understand the structural variation in Pluronic F-127 micelles after loading with different hydrophobic cargoes (alkanes, fatty acids, anticancer therapeutic agents). Different preparation methods have been applied to get a homogenous solution of samples. Temperature and concentration have been varied in near-critical micellar transition zone to observe the phase transition. SAXS (Small Angle X-ray Scattering) is used to get the scattering intensity profile of samples, and then data is processed and reduced by Foxtrot and Mantidplot software. Finally, all structural variation has investigated using core-shell hard-sphere, core-shell Hayter MSA, and core-shell Guinier Porod models. The purpose of this work is to investigate radius, thickness, SLD, volume fraction, and other structural parameters and getting a transparent idea about the micellar interaction near-critical micellar zone, which has a promising contribution to improving drug encapsulation and drug release at a controlled rate. The scattering intensity profile of samples provides strong evidence of micelle formation near CMC and CMT (critical micellization temperature). The radius of the core increases proportionally with longer alkane chain. pH value decreased with increased Linoleic acid concentration and structural parameters are fully reversible with temperature variation. For temperature-dependent samples, micelle formation has been observed around 20-30 ^{0}C and sol-gel transition around 35-40 ^{0}C.

TABLE OF CONTENTS

LIST OF FIGURES

1. INTRODUCTION

1.1 Drug Delivery System

Drug delivery is a method of administrating medicine to achieve a curative effect in humans or animals. Improving the efficacy ratio of drugs using individual drug therapy, dose titration, and therapeutic drug monitoring has become very popular because developing a new drug is time-consuming and costly. Controlled drug delivery, slow and targeted delivery are also essential components of drug delivery. [1] The performance and manufacturability of a drug depends on its physicochemical properties such as solubility, molecular weight, pH, and partition coefficient[2]. Medications can be taken by inhalation, swallowing, absorption through the skin, or injection. Among all methods, oral administration or swallowing is most used, but this delivery system is complex for some medication because of the urgency of ensuring bioavailability during administration. Polymeric micelles can overcome oral delivery limitations and perform as a drug carrier to enhance drug absorption. These micelles can protect the drug from the harsh environment of the GI tract, release the drug at a targeted site at a controlled rate, and prolong the residency time of medicine. Most importantly, polymer micelles are the potential carrier for poorly water-soluble drugs to achieve good oral adsorption. [3]

1.2 Micellar Properties of Pluronic F-127

Pluronic F-127, (PF-127) is a nonionic triblock copolymer (PEO-PPO-PEO) developed from the self-assembly of two monomeric units of Polyethylene Oxide (hydrophilic) and one Polypropylene Oxide unit (hydrophobic) which shows amphiphilic characteristics[4]. Due to its chemical structure, Pluronic F-127 can be useful as surfactants, stabilizers, solubilizing and coating agents [5] (see Figure 1). According to previous studies, the efficiency of drugs encapsulated in micelles

is better than free drugs because of the slow dissolution of the drug in the blood circulation system. [5] Using different pH buffers and micelle concentrations, PF-127 can have sol-gel transition around body temperature (32 -37 °C), promising for thermo-gel formation. Previously, for in-vitro studies, Pluronic F-127 thermo-gel released 90% of the drug at pH 5 and about 55% at pH 7.4, indicating stability at pH 5 [4]. Pluronic F-127 contains 70% of PEO, which contributes to its hydrophilicity, and it becomes gel at room temperature with 20-30 wt% concentration.[6] Pluronic F-127, also known as Poloxamer 407 is considered a potential candidate for drug carriers due to drug encapsulating structures that may be formed. It is favorable engagement with physiological barriers to drug passage and adsorption properties, which play a vital role in drug release rates and formulation stability [7]. Previously, buffered F127 has been prepared to investigate ordered mesoporous silica (OMS) near pH 5, the isoelectric point of F127. Silica wrapped around uncharged F127 particles (Silica shell, F127 core) self-assembled in a cubic close-packed organization with an increasing amount of silica.[8]

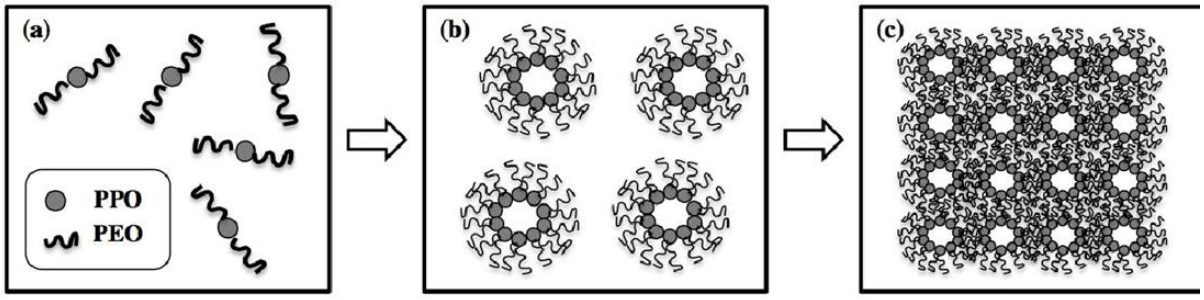

Figure 1. (a) Pluronic F-127 unimers in a solution [9] shows Pluronic F-127 (PEO-PPO-PEO) triblock copolymer in a solution where PPO is hydrophobic and PEO is hydrophilic. (b) Pluronic F-127 micellar formation. Core of micelles are made of hydrophobic PPO and outer surface is made of hydrophilic PEO. (c) Micelles arranged in cubic structure.

The drug delivery compatible self-assembled micelle structures of Pluronic F127 have been observed above critical micelle concentration 0.2%-0.8% wt concentration with varying

temperature. For Pluronic F-127, critical micelle concentration (CMC) is around 0.7% at room temperature 25 0C. [10] Also, an increase of Pluronic F -127 (molecular weight 11,500) concentration can lower the drug release rate, while an increase in temperature increases the release rate. It has been observed in past studies that the most important factor in controlling drug release from Pluronic F 127 is the physicochemical properties of the solute and the substance able to pass through or into a polymer known as permeant. [11]

The focus of this work is to investigate the variation of structural properties of Pluronic F-127 micelles with different types of permeants, including alkanes (Hexane, Octane, Decane, Dodecane), fatty acids (Oleic acid and Linoleic acid), anticancer chemotherapeutic agent Paclitaxel. Also, the purpose of this work is to analyze the impact of temperature and concentration of these hydrophobic cargoes on micelle their stability and suitability for drug delivery applications.

1.3 Alkane Interaction with Micelles

Alkanes are hydrophobes (low water-soluble molecules) with long-chain alkyl chains that do not interact strongly with water molecules. A particular interaction can be defined using an example of a mixture of fat and water. Fat molecules tend to clump up together than distributing themselves in a water medium. It follows Gibb's formula, where a change in enthalpy indicates the mix of hydrophobe and is entropy.

$$\Delta G = \Delta H - T\Delta S$$

When alkane drops in water, hydrogen bonds of water break to give room to hydrophobes, and this causes heat in the system. If enthalpy change is slightly positive, then it indicates spontaneous hydrophobic interaction. Hydrophobic interaction allows phospholipid bilayer membrane to

decrease in surface area and reduce undesirable interaction with water. Hydrophobic interaction strength increases with temperature increase. However, hydrophobic interactions will denature at an extreme temperature. Also, molecules with the most significant number of carbons will have the most robust hydrophobic interactions. The hydrophobic effect of an aliphatic organic molecule and linear carbon chain can produce the most extensive hydrophobic interaction [12]. At below or above CMC, alkane solubility experiences a linear increase with increasing biosurfactant concentration. Stronger molar solubilizing ratio (MSR) below CMC has been observed and it follows the order decane > dodecane > tetradecane > hexadecane at monoRL concentration below CMC. Decane water solubility is 0.37 uM, CMC of biosurfactant in presence of n-alkanes is 150 uM ; Dodecane water solubility 0.02, CMC of biosurfactant 155um. (In the absence of alkane 166 uM). MonoRL has a pKa of 5.6, which supports the assumption that monoRL is anionic.

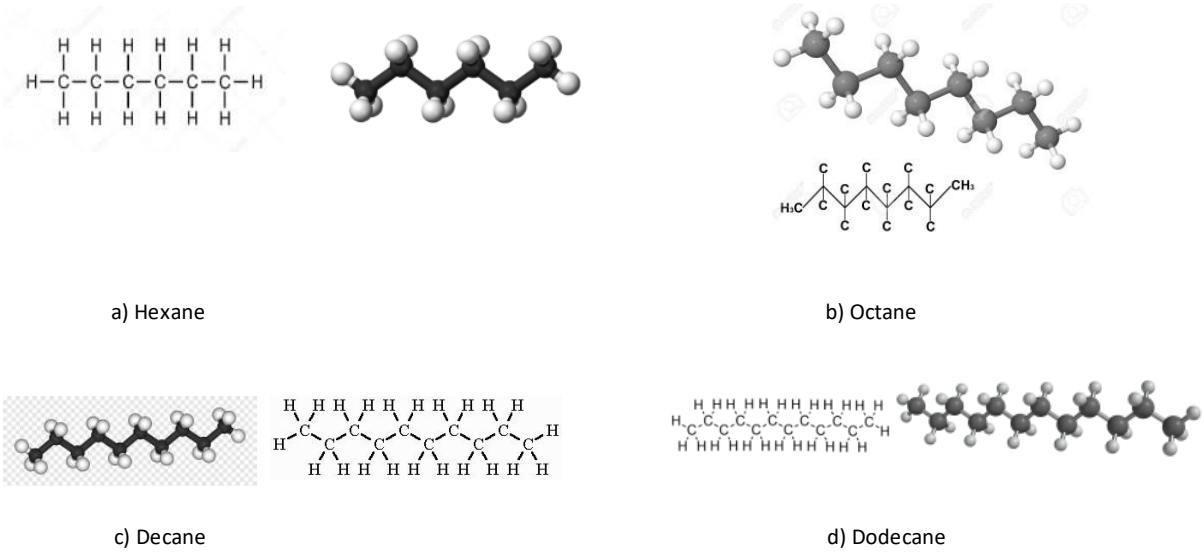

Figure 2. Chemical Structures of Alkanes a) Hexane (C_6H_{14}) b) Octane (C_8H_{18}) c) Decane ($C_{10}H_{22}$) d) Dodecane ($C_{12}H_{26}$)

Aggregates size at monoRL concentration of CMC decreases following the order decane ≈ dodecane > tetradecane > hexadecane. [13] **Figure 2** shows the chemical structures and molecular

formula of the alkanes used in this study. Structures indicate the increase of the C-H bond with an increment of alkane numbers. The molecular weight of Hexane, Octane, Decane, and Dodecane is increasing with alkane numbers.

1.4 Fatty Acid Interaction with Micelles

Micelles are amphiphilic co polymer which have hydrophobic core to accommodate hydrophobic drugs, whereas the hydrophilic shell develops colloidal stability. Because of the unique feature of amphiphilic co polymers, these materials have been studied in detail for biomedical application. Rahul et al. studied Oleic acid-carboxymethyl chitosan (OA-CMCS) conjugate as carrier for poorly water-soluble drugs and results demonstrated promising characteristics of OA-CMCS enhancing biopharmaceutical performance. [14]

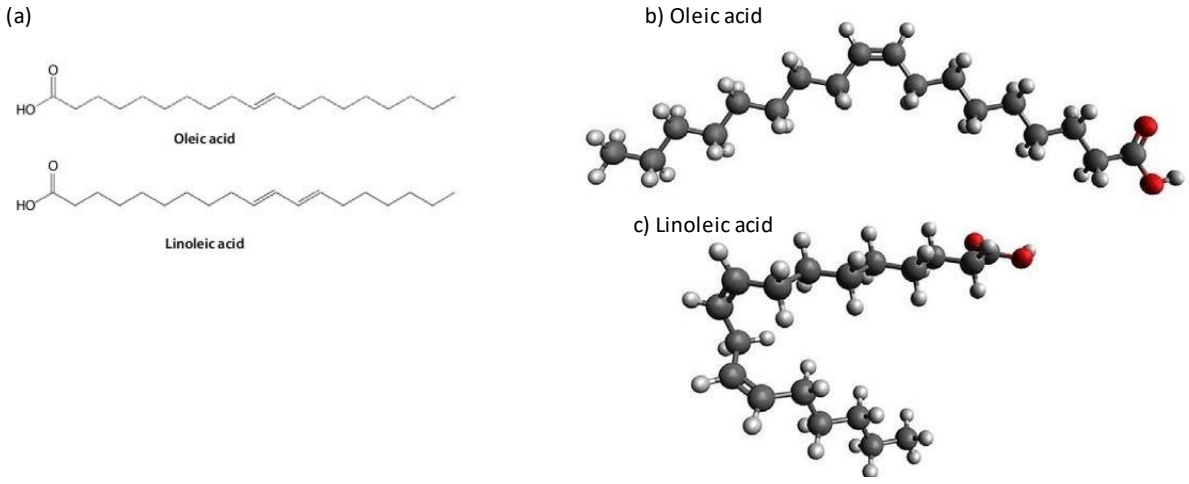

Figure 3 Chemical Structure and molecular structure of Oleic acid and Linoleic acid ($C_{18}H_{32}O_2$)

The vital difference between Oleic acid and Linoleic acid is their structure. Oleic acid ($C_{18}H_{34}O_2$) is a monounsaturated fatty acid with one double bond and Linoleic acid ($C_{18}H_{32}O_2$) is a colorless

polyunsaturated omega-6 fatty acid with two or more double bonds. Oleic acid has molecular weight 282.5 g/mol, boiling point 360 ^{0}C, melting point 29.2 ^{0}C and Octanol Partition Coefficient 7.64. Linoleic acid has boiling point at 365 ^{0}C at 16 mm Hg , melting point at -8.5 ^{0}C and Octanol-Water Partition Coefficient (log P) 7.05. Both fatty acids are insoluble in water and freely soluble in acetone, benzene, ethyl ether and ethanol. [15][16][17]

1.5 Paclitaxel Interaction with Micelles

Paclitaxel is a anticancer theraputic agent which plays a cruicial role in ovarian, breast and lung cancer therapy. Paclitaxel, also known as Taxol has molecular formula $C_{47}H_{51}NO_{14}$ and molecular weight 853.9 g/mol. This water insoluble drug has melting point at 216-217 ^{0}C and Octanol Partition coefficient (logP) is 3. If stored at room temperature, Paclitaxel starts decomposing slightly after 30 days.[18] Local tumor treatment by using controlled release of polymer encapsulated drugs wich are placed in target disease region can result in high drug concentration with systematic release and low toxicity.

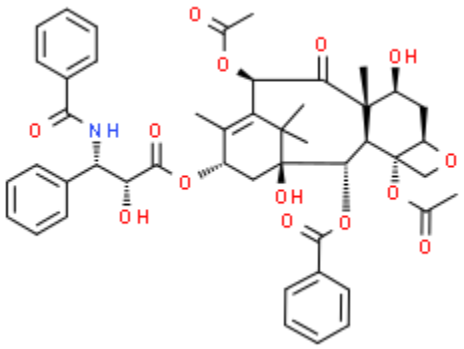

Figure 4 : Chemical Structure of Paclitaxel (C47H51NO14)

Considering these aspects, Paclitaxel loaded with Pluronic F-127 micelles can be a promising candidate for therapeutic treatment. Previous investigation revealed, 30-40% Paclitaxel releases

within 20 hours at 37 ^{0}C and 80% of the drug releases in 3 days if encapsulated in Pluronic F-127 micelles. Also, Paclitaxel is in amorphous or molecular state, which disappeard in the polymer after encapsulation. Paclitaxel loaded Pluronic F-127 provide low viscosity solution at room temperature and encounter sol-gel transition at 33-37 ^{0}C. Pluronic F-127 micelles and Paclitaxel combination shows controlled drug release ability and has great portential for local delivery of medicine in solid tumors. [19]

1.6 Critical Micellar Zone of Pluronic F-127

Critical micellar zone depends on two main components- Critical micelle concentration (CMC) and critical micelle temperature (CMT). CMC is an important property of surfactant which is known as a concentration above which surfactant molecules aggregates and starts to form thermodynamically stable micelles. Surface tension at different concentration can give an idea about CMC value. Surface tension decreases with increasing concentration of surfactant below the CMC as the number of surfactants at the interface increases. In contrast, surface tension of the solution becomes constant above CMC because interfacial surfactant concentration becomes constant.[20]

Temperature plays a vital role in the structure of micelles as below the critical micellization temperature (CMT), Pluronic F-127 molecules forms monolayer and contribute to an increase in adsorbed layer thickness. The CMC and CMT values of Pluronic F-127 is a function of molecular weight, PPO/PEO composition, concentration, or temperature. The addition of water can also affect the micelle formation and structure. Previous studies has shown that CMT for 0.01% Pluronic F-127 is 38 ^{0}C and CMT decreases to 24 ^{0}C when concentration is increased to 1% [21] and CMC value is around 0.7% at 25 ^{0}C. [10]

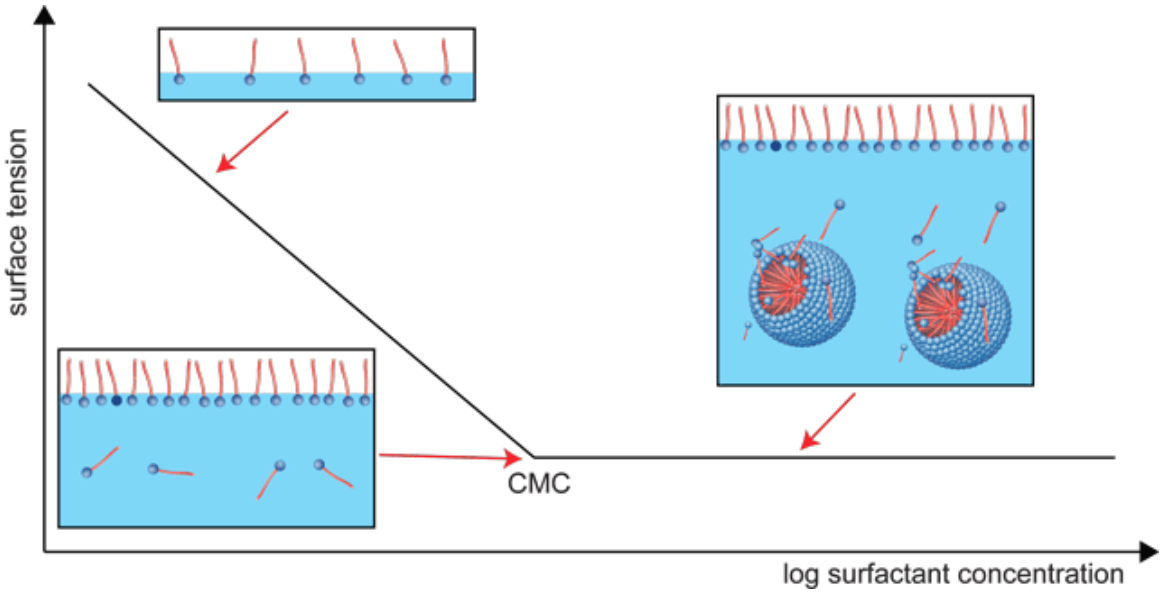

Figure 5 Surface tension as a function of the surfactant concentration. The role of critical micellar concentration and surface tension in forming stable micelles is displayed. [20]

2. SMALL ANGLE X-RAY SCATTERING (SAXS)

2.1 Introduction

SAXS is a useful technique to determine the average size and shape of nanosized particle systems. In SAXS, x-ray are scattered elastically by the electrons of molecules and the low-angle scattered intensity is measured as a function of scattered angle[22]. In the case of elastic scattering, there is no transfer of energy between the incident and scattered photon and hence there is no wavelength difference as in Compton scattering. Elastic scattering produced by visible light and x-ray are respectively called Rayleigh scattering and Thomson scattering[23]. When the x-ray strikes bound electrons, these electrons oscillate and emit radiation at the same frequency as the x-ray. The scattered waves from neighboring atoms also have the same frequency producing “coherent scattering”. The constructive interference of these coherent waves at the detector is related to the information of the structure of particles. We can obtain information of particle morphology by

analyzing the angle-dependent intensity of the scattering pattern. Depending upon the angular range SAXS can resolve the particle of size from 1nm to 150nm and can be extended on both sides by using Wide-Angle X-ray Scattering (WAXS) and Ultra Small Angle X-ray Scattering (USAXS), respectively. Like electron microscopy, X-ray scattering makes use of the variation of a sample's electron density to generate contrast. SAXS measurement is considered faster but SAXS data displays structure in a lower resolution than electron microscopy. Both techniques provide complementary information; however, the former yields real space images while the latter provides reciprocal space data[24]. As "reciprocal" implies a spatial variation of electron density at nanometer length scales (larger distance) will scatter an X-ray beam to low angles while variations at the atomic scale will scatter to high angles. To get the desired properties of nanoparticles, controlling the size of nanoparticle is a necessity. It is not possible to control particle size if we are unable to quantify the sizes of nanoparticles. SAXS has the advantage over other techniques as this method allows to study material structures at large dimensions, or small angles with a wide variety of sample type including colloidal suspension. Conversely, wide angle X-ray scattering (WAXS) is used to measure the scattering intensity at large angles, or small dimensions.

Another advantage of using SAXS is that prior knowledge about form of a particle size distribution is not needed, which is hard to assume before analyzing the sample. [25]

2.2 SAXS Instrumentation

SAXS (Small Angle X-ray Scattering) instruments contain an X-ray source, a collimation system, a sample holder, a beam stop and a detector. Cu x-ray has been used as source because of its low divergence, monochromatic beam. Collimation makes the beam parallel, the beam stop has been used to protect the detector from high intensity flux of non-scattered x rays, and finally detector records the scattering intensity which is used for data processing and analyzing.

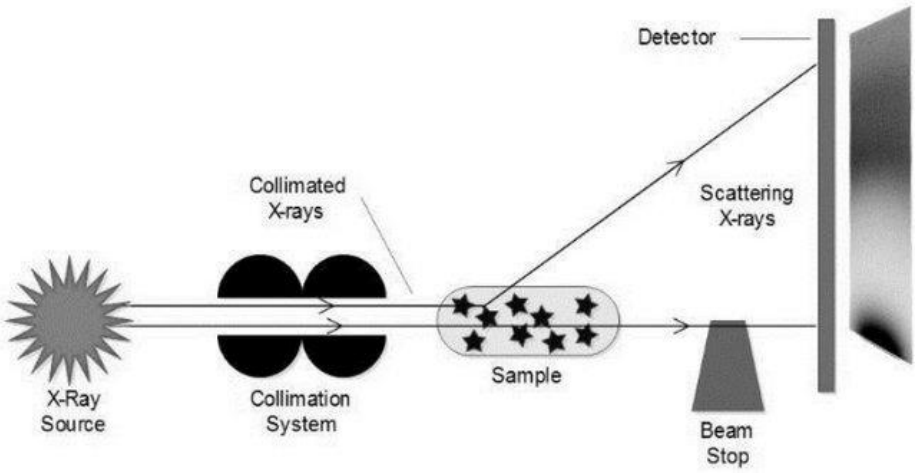

Figure 6 : Schematic Diagram of the Components of SAXS instrument. [26]

2.2.1 X-ray Source

Predominantly, a rotating anode or microfocus x-ray source, a sealed x-ray tube is used as a source in SAXS instrument

.

Figure 7 : X-ray source GeniX 3D Cu High Flux

For this study, microfocus source named “GeniX 3D Cu High Flux” has been used. [27] This copper source has a wavelength of 1.5419 Å along with system power consumption of 30 Watts, 0.6mA, 50 kV.

2.2.2 The Collimation System

Collimation system is SAXS is very important for separating incoming beam from small angle scattered radiation. Our SAXS instrument uses slits in collimation system to control the beam size and divergence of incoming beam. In general x-rays from source are not monochromatic, they are made monochromatic using multilayer optics. Without collimation it is difficult to differentiate between low scattering intensity from sample and high intensity from direct beam. Bragg’s law can connect the angle θ at which x-ray of wavelength λ falls on surface with a distance d towards obtaining a constructive interference. Bragg’s law can be written as $2d\sin\theta = n\lambda$. Here n is an integer and can be n=1,2,3…n

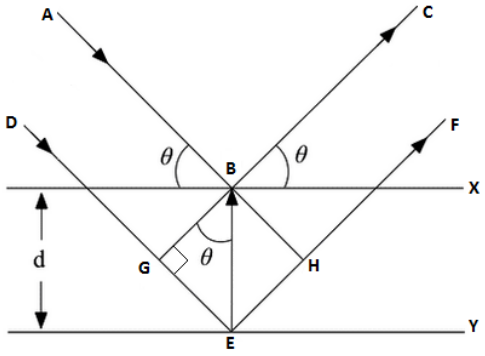

fig: Bragg's Law

Figure 8: Bragg’s Law. [28]

2.2.3 The Sample Holder

Sample holder is a crucial part of SAXS instrument as sample itself cannot stand the necessary vacuum environment needed for low background scattering. Also, environmental changes such as

pressure, temperature, strain etc can be introduced due to research purposes. Therefore custom made sample holders with variants of commercial setup has been used.

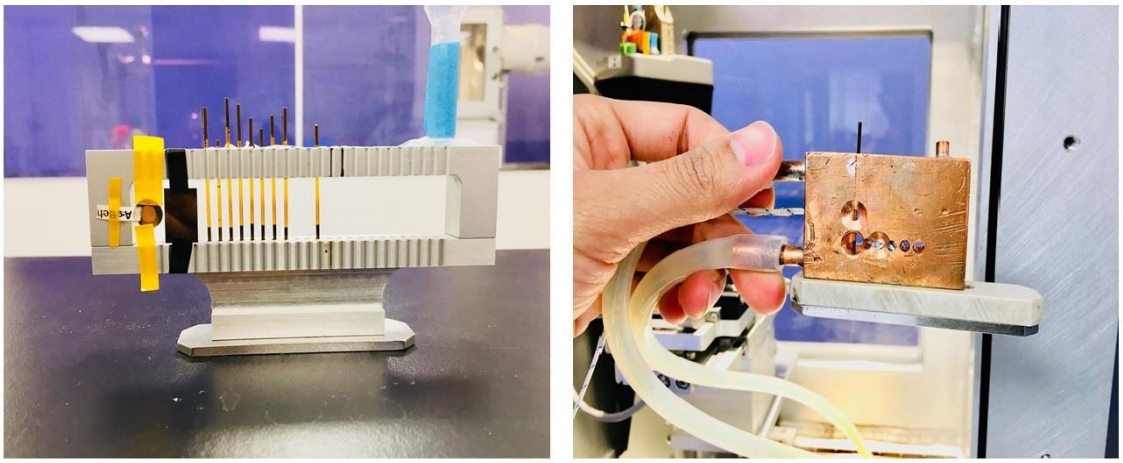

Figure 9 a) Regular sample holder b) Sample holder for temperature dependent experiment.

2.2.4 The Beam Stop

The beam stop prevents the rigorous direct beam from hitting the detector. Usually, two kinds of beam stop are used to avoid the problem of overshadowing weak signals of the samples from strong background signals. One kind is made of dense materials which blocks off direct beam completely, another kind is made of transparent material. Transparent material made beam stop is used in our lab because the intensity of direct beam can be monitored simultaneously along with sample scattering and beam intensity can also be enervated for safety of the detector.

2.2.5 The Detector

There are four types of detectors (wire detector, CCD detector, imaging plates and solid-state (or CMOS)) for SAXS instrument. We used a solid-state detector named Dectris Pilatus 3R 200-A. This detector works for wide range of x-ray application. It has sensitive area of 83.8 mm×70.0 mm and pixel size 172 µm × 172 µm. [29]

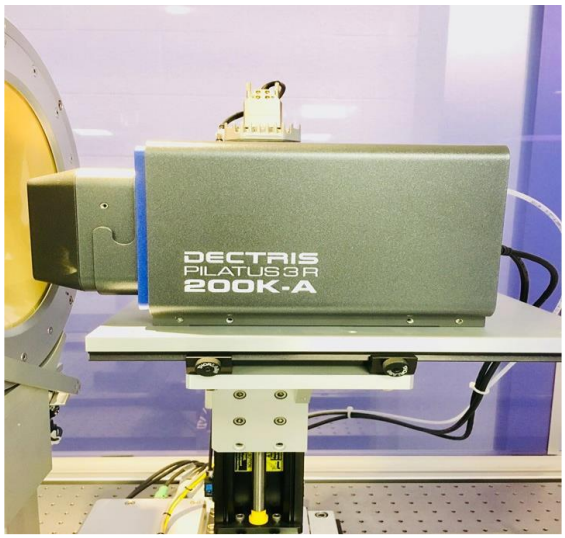

Figure 10 Dectris Pilatus 3R 200-A

2.3 SAXS Theory

SAXS technique calculate the differential scattering cross section per unit volume $\frac{d\sum(q)}{d\Omega}$, related to Fourier transform of the electron density distribution of a material. Waves scatter more for samples with higher electron density. If volume of a particle is V_1, scattering length density ρ_1 then total scattered intensity can be written as,

$$I_1(q) = I_0.\rho_1^2.V_1^2.P(q) \qquad (1)$$

Here, P(q) is the form factor of the particle. When this particle with scattering length density ρ_1 immersed into another matrix of ρ_2, then scattered intensity becomes,

$$\Delta I_1(q) = I_0.\Delta\rho^2.V_1^2.P(q) \qquad (2)$$

N number of identical particles will cause an intensity of $\Delta I(q) = N.\Delta I_1(q).S(q)$ (3)

Here, $\Delta\rho = \rho_2 - \rho_1$ and S(q) is known as structure factor which considers the particle position relative to each other. As SAXS signal increases strongly with particle volume, there are two main

consequences of above equation (2). As volume becomes larger, one dispersion can contain one million particles of one size and a single particle with another size. In that case, sample will produce scattering pattern from both sizes. Another crucial consequence is that voids and material particles in a matrix gives same intensity. Monodisperse samples are rare, because highly unlikely N particles in a sample are identical to each other. [30]That is why introducing polydispersity in calculation is important. If we assume dilute particle dispersion, S(q)=1 then

$$\Delta I(q) = I_0 \sum_{i=1}^{N} \Delta\rho_i^2 . V_i^2 . P_i(q) \qquad (4)$$

2.3.1 Form Factor P(q) and Structure Factor S(q)

As one particle is made of many atoms, the scattering of one particle can be explained by the interference pattern of scattering amplitudes from every electron inside a particle which occurs at the detector plane. The measured intensity at the detector position is the square of these amplitudes that results in an interference pattern. This pattern oscillates in a fashion that is characteristic for the shape of the particle which is called form factor. The form factor describes individual particle scattering, and different particle shapes will give a different form to $P(q)$.

The distances of particles relative to each other come into the same order of magnitude as the distances inside the particles when particles are closely packed. The interference pattern will therefore contain contributions from neighboring particles as well. Structure factor $S(q)$ considers the interparticle interactions. This is useful in describing the nature of interaction between the particles.

3. EXPERIMENTAL METHOD

The SAXS instrument, Xeuss 2.0 HR SAXS/WAXS system, in NICE^2 Lab at The University of Texas at El Paso has been used for scattering measurement. One of the main features of Xeuss is that the sample-to-detector distance is long and changeable which is convenient to achieve very low q_{min} value down 0.025nm^{-1} with high angular resolution. Based on experimental need, all components of SAXS are controlled by software. It is equipped with a uniquely motorized software virtual detector mode. To obtain a large effective radiation, two dimensional images taken at different positions are automatically recombined.

Figure 11 : Xeuss 2.0 SAXS instrument

3.1 Materials

Pluronic F-127($C_{572}H_{1146}O_{259}$) was purchased from Sigma-Aldrich. It is a powder like bioreagent with a molar molecular weight of 12600g/mol. Hexanes [C_6H_{14}] was bought from Fisher

Chemicals, n-Octane [C_8H_{18}] (Extra dry, Acroseal) and N-Decane [$C_{10}H_{22}$] from Acros Organics, n-Dodecane [$CH3(CH2)_{10}CH_3$] were bought from Alfa Aesar. Also, Fatty acids- Linoleic acid [$C_{18}H_{32}O_2$] was bought from Sigma-Aldrich and Oleic acid [$C_{18}H_{34}O_2$] is from Alfa Aesar. Paclitaxel [$C_{47}H_{51}NO_{14}$] in a form of crystalline solid with molecular weight 853.906 g/mol which is known as a chemotherapy medication was also bought from Alfa Aesar. Kapton tube (polyimide tube), epoxy, syringes, weighing machine, furnace, ultrapure milliQ water, acetone, kim wipe, glass containers and vials were provided by Nanomaterials, Interfaces, and Confinement for Energy and the Environment ($NICE^2$) Lab.

3.2 Sample Preparation

A very small amount of sample (10-20 µL) is needed for SAXS measurement, but it is difficult to prepare samples in such low quantity and chances of error in measurement is higher. So, it is convenient to prepare relatively large amount of sample around 2-5 mL of sample. Pluronic F-127, alkanes, fatty acids and drugs were weighted by using balance machine provided by $NICE^2$ Lab and syringes (0.5 mL) have been used to ensure the accurate measurement. After preparing the solution, all samples have been mixed using magnetic hot plate for 60 minutes at 60 ^oC. Then samples are sonicated and heated at 60 ^oC for an hour using ultrasonication bath. Fatty acids with Pluronic F-127 solutions have been stored at low temperature about -20 ^oC and other samples have been stored at room temperature.

Freshly made samples have been injected inside epoxy sealed Kapton tubes. Epoxy filled empty Kapton tubes need to be left for 24hours before injecting sample inside it. Then Sample filled Kapton tubes are sealed with hot glue and sandpapers are used to set the hot glue on the top of the tube properly. Also, pH buffer solutions of pH 4.01, 7.00 and 10.00 have been used to calibrate pH meter before measuring pH of the samples. Plenty of samples have been prepared with different

concentration to get the most convenient output during this investigation. But 5% wt concentration of Pluronic F-127 is constant for all the samples measured.

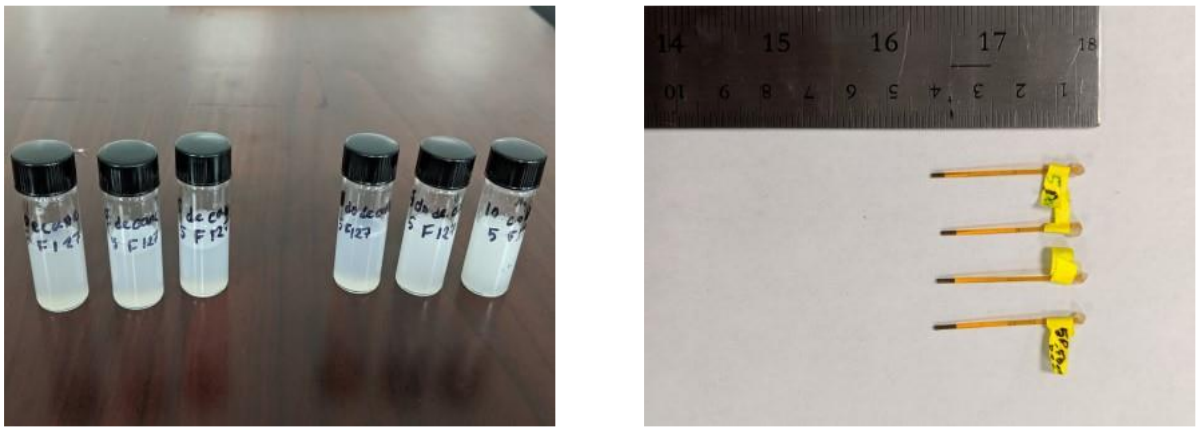

Figure 12 a) Freshly prepared samples in vial b) Sample filled Kapton tubes ready for SAXS measurement.

3.3 System Control and Data Acquisition Software

Complete monitoring of data acquisition parameters is done by the Xeuss 2.0 control and data acquisition software interface specfe. Specfe is based a Certified Scientific Software named SPEC. Different kind of settings for collimation, sample stages, detector and beam stop alignment are available in this software.

3.4 Sample Measurement

SAXS measurement needs two sets of measurement for obtaining required information of a sample. One measurement is for only background and other one for sample with background. In this study, we have used water as background and solution of micelle/fatty acid/alkane/drug as sample which includes water as a solvent. All measurements have been done in vacuum with sample-to-detector distance 1209 mm. Acquisition setting have been set to virtual detector mode

and collimation high flux and high resolution. The slit positions are 1.20×0.60 for slit 1 and 0.80×0.50 for slit 2. Each sample exposed to the x-ray for 30 minutes.

3.5 Data Processing and Analysis Software

Foxtrot (version 3.3.4) and Mantidplot (version 4.2.0) software are used for data processing and analyzing, respectively. The Foxtrot software is designed to allow easy processing of single or large sets of two dimensional (2D) images, masking the raw data to get rid of the beam stop, subtraction and one-dimensional integration (1D) in polar coordinates or azimuthal projection over complete pattern or on a predefined region of interest. Foxtrot easily exports masked data into a convenient .Dat format for data reduction purpose. After processing .Dat files in Mantidplot software, reduced data can easily be exported to advanced data analysis packages as SasView or ATSAS. SasView (version 4.2.2) software has been used in this study for data analysis purpose.

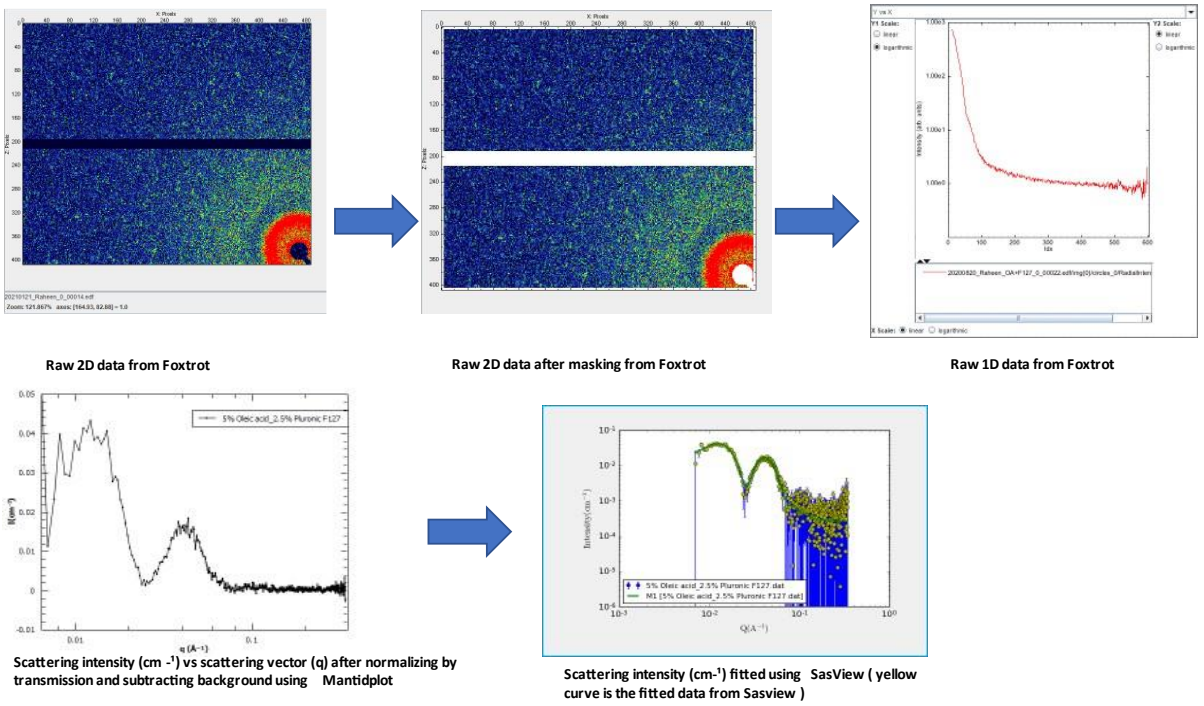

Figure 13 Steps of data processing and analyzing using Foxtrot and Mantidplot.

3.6 Data Reduction using Foxtrot

Conversion of 2D raw data obtained from SAXS instrument is important for data reduction. Foxtrot software is used to convert 2D raw data into 1D raw data which are fully reduced using Mantidplot. Foxtrot gives the value of transmission and intensity of sample and background. Mantidplot is used for full reduction because it is not a manual software like Foxtrot. It uses python script to complete the data reduction process accurately and other functions like scaling, normalizing, calibration etc. can be done using python script.

3.7 Data Reduction using Mantidplot

Raw data from SAXS measurement are obtained in Edf format which needs to be masked at first in order to get rid of unwanted signals. Then this data should be reduced before fitting. Data reduction is done by Foxtrot and Mantidplot. Information needed to calculate transmission coefficient of each sample are mentioned below:

1. Direct and scattering beam of both sample and background
2. Direct and scattering beam of empty container
3. Direct and scattering beam of empty instrument
4. Direct and scattering beam of glassy carbon.

Intensity of the samples can be obtained from following equation,

$$I(Q)(cm^{-1}) = A.\left(\frac{Isample}{tr.sample \times t} - \frac{Ibuffer}{trbuffer \times t}\right)\frac{1}{d} \qquad (5)$$

Where, A is the absolute Intensity calibration which is a scaling factor obtained by matching the original glassy carbon intensity with the glassy carbon intensity obtained from the SAXS instrument, I_{sample} is the raw intensity of sample, I_{buffer} is the raw intensity of buffer, tr_{sample} is the

transmission of sample, tr_{buffer} is the transmission of the buffer, t is the exposure time and d is the sample thickness.

The transmission of sample or buffer is defined as, $T=I_s/I_0=e-\mu d$ (6)

Here, I_o is the incident intensity of X-ray, I_s is the scattered intensity and μ is the linear attenuation coefficient and d is the thickness if sample.

3.8 Data Fitting Using Sasview

Sasview is an open-source data analysis software which analyzes small angle scattering data. Reduced data from Mantidplot is fitted in Sasview using form factor P(q) and structure factor S(q). There are several built in models available in the software but if data is not fitted with provided models then there is also option for customizing own model to get the best fitting. Most of our samples are fitted with core shell sphere Hyter MSA, core shell hard sphere and core shell hardsphere with Guinier Porod. Three models have been used in this study for purpose of fitting data.

- Core Shell Sphere- Hard Sphere (Alkanes-prepared at 60 ^{0}C, Pluronic F-127, Temperature dependent Fatty acids and Alkane)
- Core shell Sphere- Hayter MSA (Alkanes- prepared at room temperature, Fatty acids- Prepared at room temperature and 60 ^{0}C)
- Core Shell Sphere- Guinier Porod. (Paclitaxel- Temperature dependent)

3.8.1 Core Shell Sphere- Hard Sphere Model

This model calculates the scattering from a fractal structure with a primary building block of core-shell spheres. This calculates the form factor P(q) for a monodisperse spherical particle with a core

shell structure. The form factor is normalized by the total particle volume. This model can be used to determine aggregated particles or vesicles.

$$I(q) = P(q)\,S(q) + \text{Background} \qquad (7)$$

Where P(q) is the core-shell form factor and S(q) is the structure factor.

$$P(q)=\phi/V_s[3V_c(\rho_c-\rho_s)\,[\sin(qr_c)-qr_c\cos(qr_c)]/(qr_c)^3+3V_s(\rho s-\rho_{solv})[\sin(qr_s)-qr_s\cos(qr_s)]/(qr_s)^3]^2$$

&

$$S(q)=1+[D_f\,\Gamma(D_f-1)]/[1+1/(q\xi)^2]^{(Df-1)/2}\sin[(D_f-1)\tan^{-1}(q\xi)]/(qr_s)^{Df} \qquad (8)$$

Here ϕ is the volume fraction of particles, V_s is the volume of whole particle, V_c is volume of core, ρc, ρs, and $\rho solv$ are the scattering length densities of the core, shell, and solvent respectively, r_c and r_s are the radius of the core and the radius of the whole particle respectively, D_f is the fractal dimension, and ξ the correlation length. Polydispersity of radius and thickness can be determined through this model as well. This model does not allow for anisotropy and thus the 2D scattering intensity is calculated in the same way as 1D, where the q vector is defined as

$$q = \sqrt{(q_x^2 + q_y^2)} \qquad (9)$$

Core shell sphere model can give idea of core radius, shell thickness, scattering length density of core and shell and volume fraction. Combining core shell sphere model with structure factor hard sphere, effective radius of hard sphere can be calculated. [31][32]

3.8.2 Core Shell Sphere-Hayter MSA Model

In this model core shell sphere has been combined with structure factor Hayter-Penfold Rescaled Mean Spherical Approximation (Hayter MSA). Hayter MSA is a dimensionless structure factor S(q) which calculates the interparticle structure factor for a system of charged, spheroidal objects in a dielectric medium. When combined with an appropriate form factor **P(q)**, this allows for inclusion of the interparticle interference effects due to screened Coulombic repulsion between the charged particles. This model only works for charged particle so if charge is not a necessary parameter for analysis then hard sphere can be used instead. [33]

3.8.3 Core Shell Sphere- Guinier Porod

In this research work, Guinier Porod has been used as a structure factor with core shell sphere to analyze Paclitaxel samples. This function calculates the scattering for a generalized Guinier/power law object. This is an empirical model that can be used to determine the size and dimensionality of scattering objects, including asymmetric objects such as rods or platelets, and shapes intermediate between spheres and rods or between rods and platelets. This function can be written as,

$$I(q)=\begin{cases} GQs \exp[-Q^2R^2_g/(3-s)] & Q\leq Q1 \\ D/Qm & Q\geq Q1 \end{cases} \quad (10)$$

This is based on the generalized Guinier law for such elongated objects. For 3D globular objects (such as spheres), s=0 and one recover the standard Guinier formula. For 2D symmetry (such as for rods) s=1, and for 1D symmetry (such as for lamellae or platelets) s=2. A dimensionality parameter (3−s) is thus defined, and is 3 for spherical objects, 2 for rods, and 1 for plates. S=0 has been fixed for the modelling of the samples in this study as all our samples contain spherical shape.

Enforcing the continuity of the Guinier and Porod functions and their derivatives yields

$$Q_1 = \frac{1}{Rg}\sqrt{(m-s)(3-s)}/2 \qquad (11)$$

Radius of gyration (R_g) can be determined using this function as structure factor. [34]

4.a) RESULTS FOR PLURONIC F-127 MICELLES

4.1. (a) Pluronic F-127 with different weight concentration

Pluronic F-127 micelles have been prepared with different weight concentration throughout this study and added with different kind of hydrophobes (Alkanes, fatty acids, drugs) with different concentration and temperature to investigate the structural variation near critical transition zone. According to previous work, one interparticle peak for 5% Pluronic F-127 with no higher order diffraction peak which suggests the absence of super micellar structure and increase of Pluronic F-127 concentration, leads to a shorter inter micellar distance. Yunqi et al. observed two peaks (secondary peak at q~0.057 $Å^{-1}$ and small shoulder peak at q~0.067 $Å^{-1}$) for 15% wt concentration of Pluronic F-127 which has resemblance with our finding for 20% wt concentration of Pluronic F-127. Gelation of Pluronic F-127 can be caused by face centered cubic (fcc) gel structure (compact packing by micelles) based on the ratio of peak positions of scattering intensity profiles obtained from SAXS. Water content in micelle core decreases with increasing Pluronic F-127 concentration and theoretical calculation and experimental measurements indicate that aqueous solutions show ordered structures with micellar packing and ordered structures are more sensitive to concentration and temperature. Also, solvent molecules can contribute to form ordered gel structure by polymer networks which results in water like micro viscous gel. Considering the complexity of structure, we decided to focus our studies on the structural variation of micellar

solution near critical micelle zone instead of Pluronic F-127 gel. [35] Focus of this work is to observe the phase transition as well which might be difficult to proceed with high concentration of Pluronic F-127 which forms gel at room temperature.

For this investigation, Pluronic F-127 solution has been prepared at 0.1%, 5%, 10% and 20% wt concentration. Among these samples 0.2% did not show micellar nature as critical micellar concentration (CMC) for Pluronic F-127 is around 0.7%wt concentration and 20% Pluronic F-127 became gel. Therefore, Pluronic F-127 with 5%wt concentration has been chosen for further investigation.

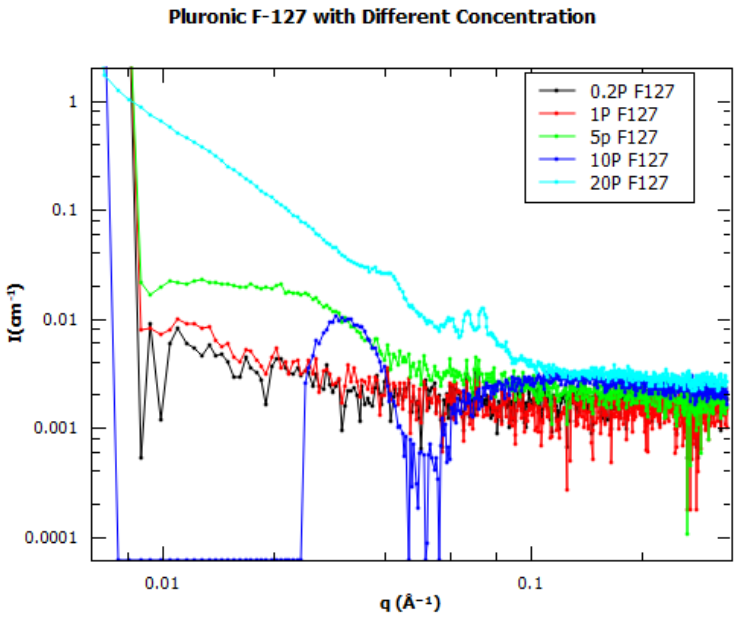

Figure 14: Reduced data of Pluronic F-127 at 0.2%, 1%, 5%, 10%, 20% wt Concentration

The figure shows reduced data plots for Pluronic F-127 at 0.2%, 1%, 5%, 10% and 20%wt concentration. Where micellar pattern has been missing at 0.2% and 1%wt concentration and most visible at 5%wt concentration. We decided to focus our studies on the structural variation of micellar solution near critical micelle zone as we want to observe the phase transition of micelles. Considering the scattering spectrums for all concentration, 5% Pluronic F-127 has been chosen for

further study and carrier for different hydrophobic cargoes. Because a higher concentration Pluronic F-127 which forms gel at room temperature might be difficult to proceed with our goal.

4.2.a) Temperature Dependent Pluronic F-127

Scattering intensity profile of 5% Pluronic F-127 has been measured in temperature range of 25 to 60 ^{0}C by SAXS instrument. Micellar formation has been observed with the increase of temperature. Peaks have been observed at q range of 0.04~0.08 Å^{-1} which has alignment with previous findings. The peak intensity increases at higher temperature. [35]

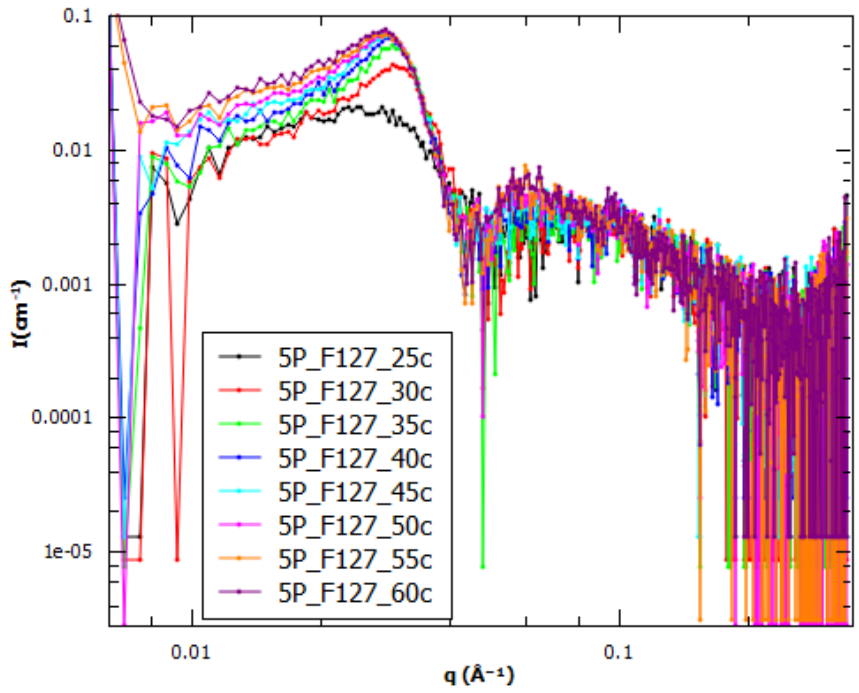

Figure 15: Scattering intensity profile for temperature dependent Pluronic F-127. Peaks are shifting to the left toward lower q region with temperature increment which indicated the distance between micelles are increasing.

4.3.a) Pluronic F-127 at Different positions of Kapton Tube

As water is not considered as a good solvent for Pluronic F-127 specially at higher temperature, it is important to measure scattering intensity from different positions of sample filled Kapton tube

to be sure of the homogeneity of the solution. 5% Pluronic F-127 prepared at 60 ^{0}C has been loaded inside a Kapton tube of thickness 0.0395 inch and measured in SAXS instrument from two different positions- top of the tube and bottom of tube. The scattering spectra shows identical results from both positions which indicates formation of a uniform homogenous solution. Discrepancy at low Q value might occur from background noise and is negligible.

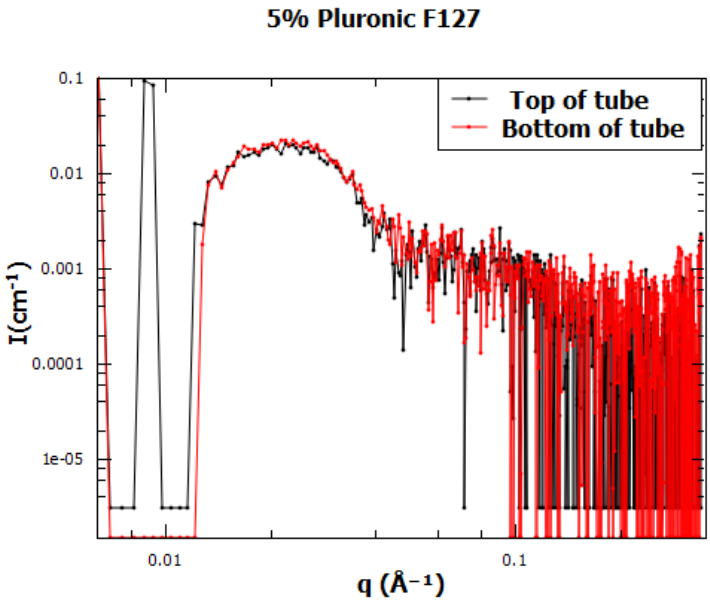

Figure 16: Scattering Spectrum for 5% Pluronic F-127 solution from different positions of sample filled Kapton tube.

4.b) DISCUSSIONS FOR PLURONIC F-127 MICELLES

4.1 b) Pluronic F-127 micelles and Core-Shell Hard sphere Fitting

Figure 17 presented core shell hard-sphere fitting for temperature dependent 5% Pluronic F-127 samples. Here, core shell sphere is the form factor and hard sphere function contributed as a structure factor. Core shell sphere described the individual particle scattering and hard sphere have explained the interparticle interaction.

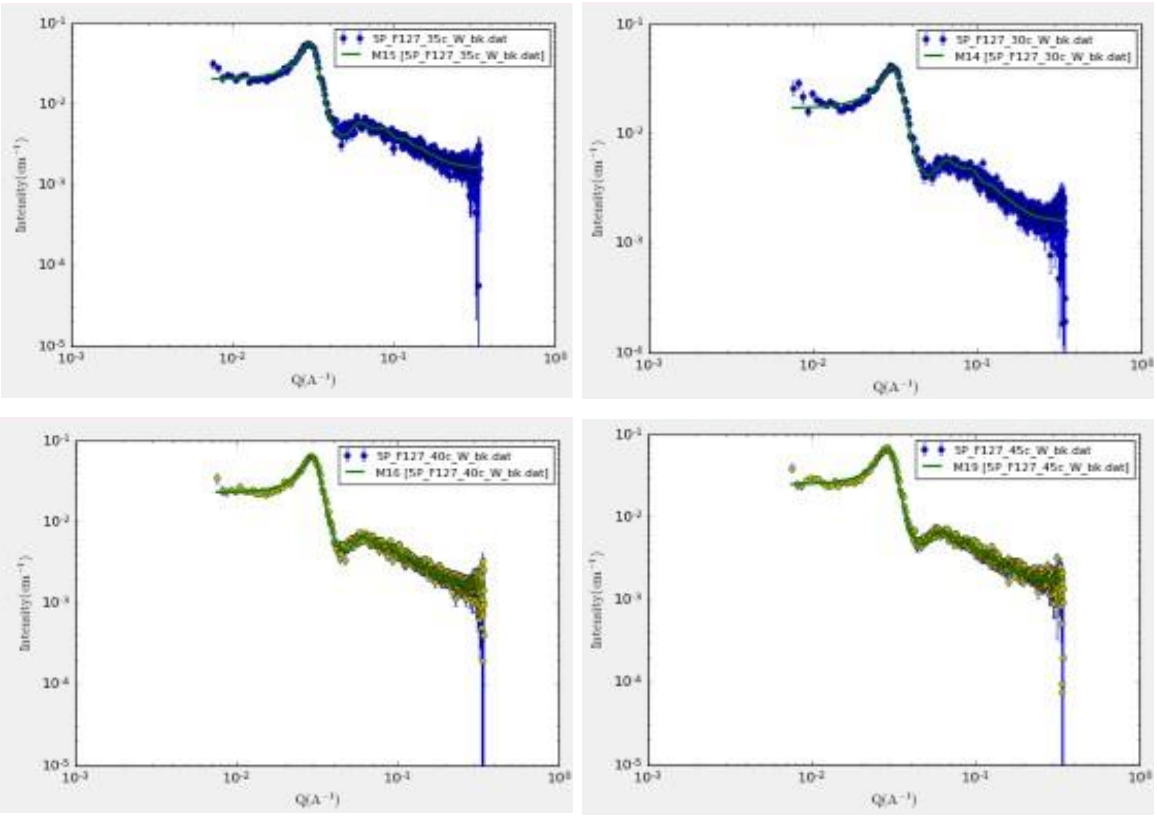

Figure 17: Core Shell Hard sphere model fitting on Pluronic F-127 micelles at Different Temperature

This fitting gives an idea about radius of core, thickness of shell, scattering length density of core and shell, volume fraction and polydispersity of the sample.

4.2.b) Discussion for Temperature Dependent Pluronic F-127 micelles

Structural properties analysis with temperature variation for 5% Pluronic F-127 have been done and **Figure 18** presents the data contrast for relevant parameters for this analysis. Thickness of shell, radius of core and SLD of core increases with temperature where SLD of shell decreased with temperature variation. Volume fraction of the sample tends to decrease after 35 ^{0}C. Kell et al. confirmed in his studies that Pluronic F-127 obtains a stable cubic crystal phase (bcc) at high temperature and remains in micellar liquid phase at low temperature.

Sol-gel transition for Pluronic 15% F-127 occurs due to increased micellar packing at low temperature region 22-30 ^{0}C and gel-sol transition occurs at high temperature region 50- 60 ^{0}C. [35]. As 5% Pluronic F 127 which is a much lower concentration than the one used in previous studies, we have observed transition due to the micellar formation around 20-30 ^{0}C and observed a second transition for sol-gel t around 35-40 ^{0}C. is visible in structural parameters obtained from sasview analysis using core shell hard-sphere model. At higher temperature dehydration of PEO contributes to reduction of volume fraction to form gel. [35] The reduction of volume fraction has been observed in 40-60 ^{0}C temperature region.

Also, the core of micelle (the PPO block) becomes hydrophilic at high temperature. So, a phase transition is confirmed for Pluronic F-127 micelles with temperature variation. In 10 to 20 ^{0}C temperature range hydrophobic interaction in the core is dominant, which causes intensity increment and results in formation of spherical micelles. Sol-gel phase transition occurs at higher temperature which results in significant increase in scattering intensity. [36] With increase of concentration and temperature, dehydration occurs at hydrophilic PEO block and solubility decreases in hydrophobic PPO block which leads to the increase of hydrophobic core size which agrees with our finding. [35]

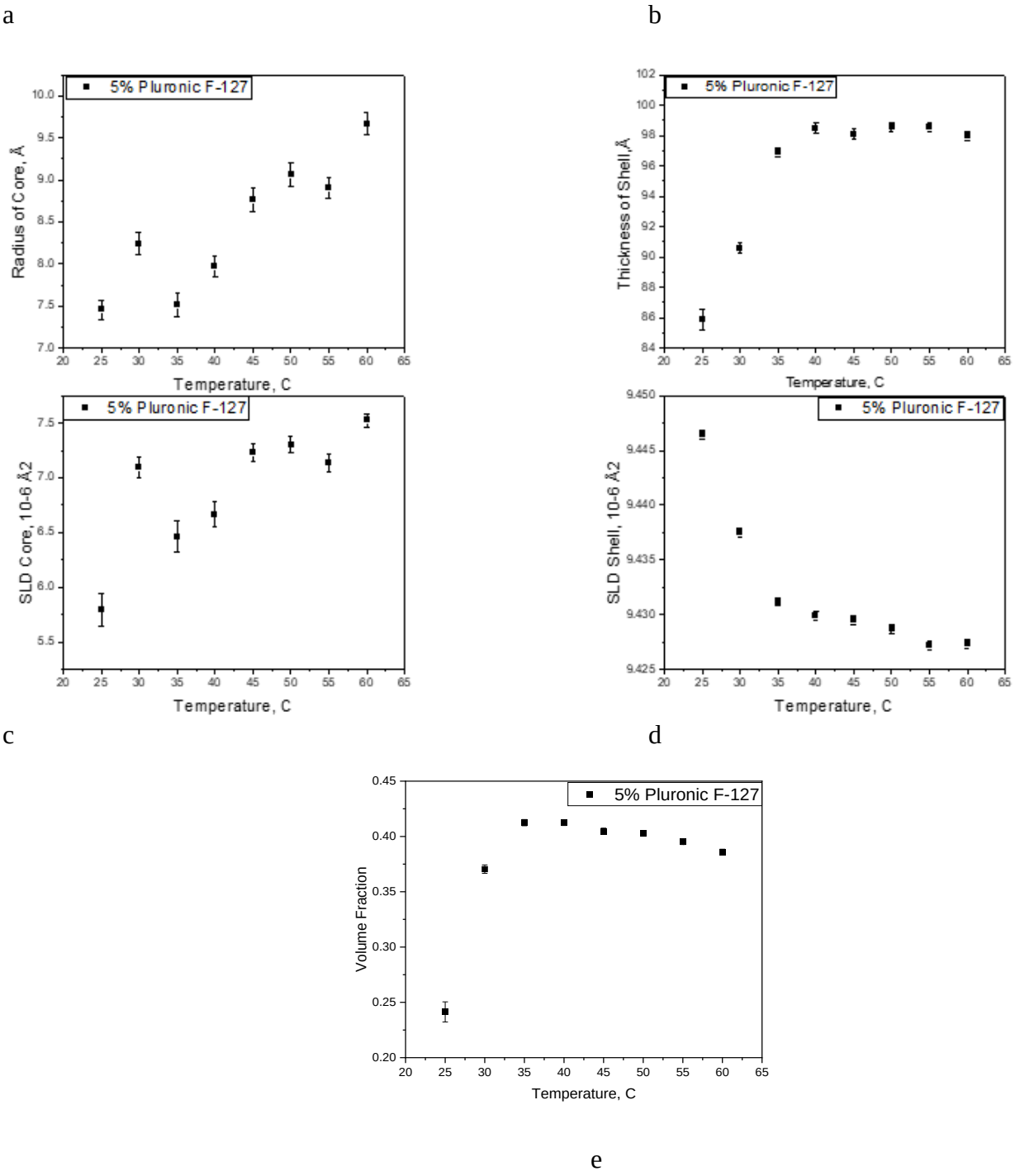

Figure 18: Temperature dependent structural properties variation of 5% Pluronic F-127 where a) shows radius of core b) thickness of shell c) SLD variation of core and d) SLD of shell and c) Volume fraction of particle with respect to temperature.

4.2.b Structural Analysis for Pluronic F-127 Micelles at Direct and Reverse Temperature Variation

Structural properties of 5% Pluronic F-127 have been analyzed using core shell hard-sphere model in Sasview software. In our study, transition is visible around 25-35 ^{0}C for 5% Pluronic F-127. Lin et al. observed that for 1% Pluronic F-127, 25 to 40 ^{0}C temperature region might behave as an intermediate region where micelles are not well formed as above 40 ^{0}C. Also, at higher concentration layer thickness might increase because of multilayer formation. [21] Therefore, differences in transition zone are not surprising as we have worked with higher concentration of Pluronic F-127. The absorbed shell thickness is comparable with the findings in previous studies and with higher concentration of Pluronic F-127, PPO core has stronger affinity to each other than that of the PEO on surface.

Previous studies shows that water is a worse solvent for Pluronic F-127 at higher temperature as the sample becomes dehydrated and diameter of micelles increases with increase of temperature which agrees with our findings. The increase in radius of core and decrease in thickness are observed in 5% Pluronic F-127. Also, a transition in thickness of shell is observed at 25 ^{0}C. SLD of core decreases with increasing temperature which indicates a loss in electron density in the core and a transition in SLD of thickness has been observed in between 25 to 35 ^{0}C.

At first, temperature has been increased from 20 ^{0}C to 40 ^{0}C with 2 ^{0}C increment and later the same sample has experienced a temperature decrease from 40 to 20 ^{0}C with 2 ^{0}C decrement. All the structural parameters including radius, thickness, SLD and polydispersity showed similar value for both cycles. This confirms that Pluronic F-127 micellar structure is affected by temperature and fully reversible.

a b

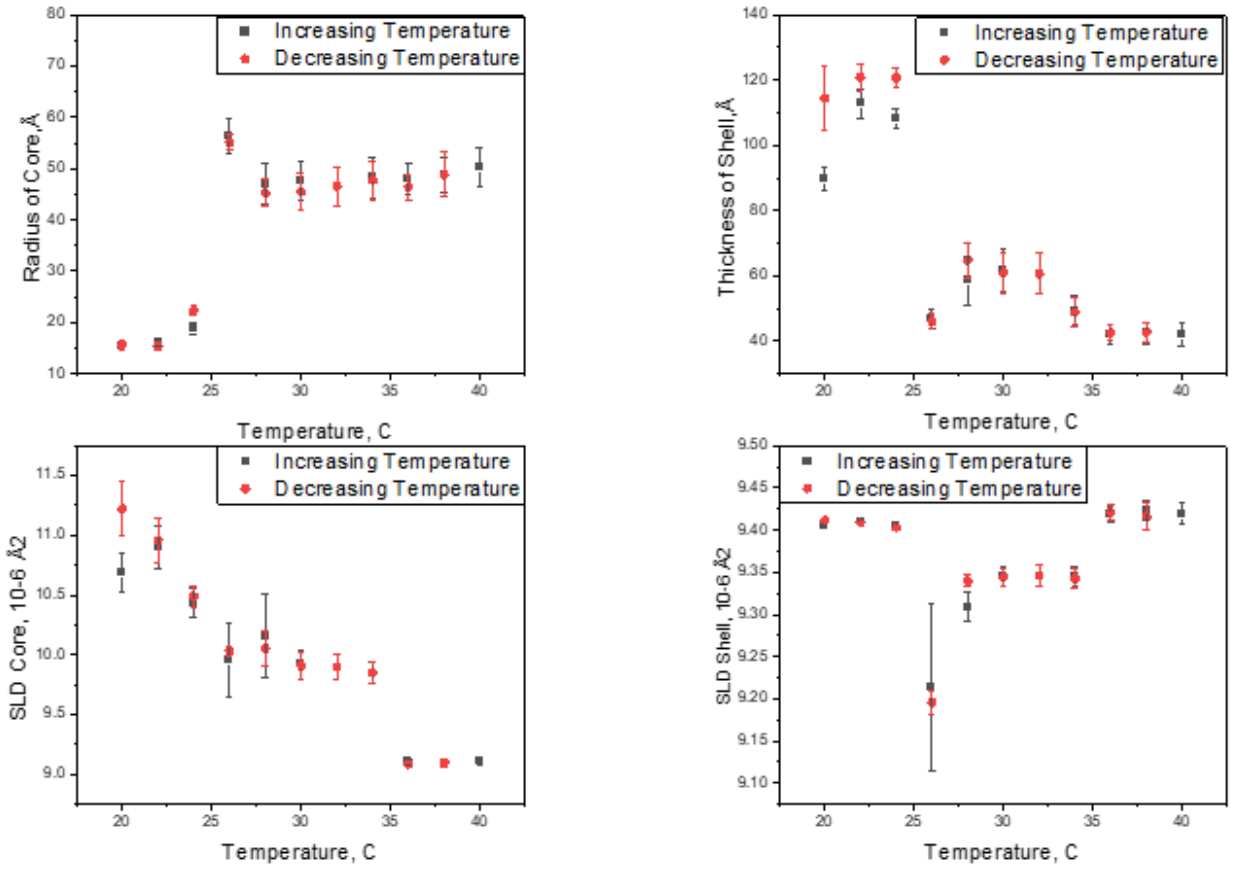

c d

Figure 19 : Structural properties variation of 5% Pluronic F-127 at direct and reverse temperature variation where a) shows radius of core b) thickness of shell c) SLD variation of core and d) SLD of shell.

Here we can see a different range for values of Pluronic F-127 than the one presented in previous section 4.2.b (Figure 19). This is because the Pluronic F-127 sample presented in this section has been shook and ultrasonicated just before the measurement. This might cause the aggregation in molecules and showed different values.

a b

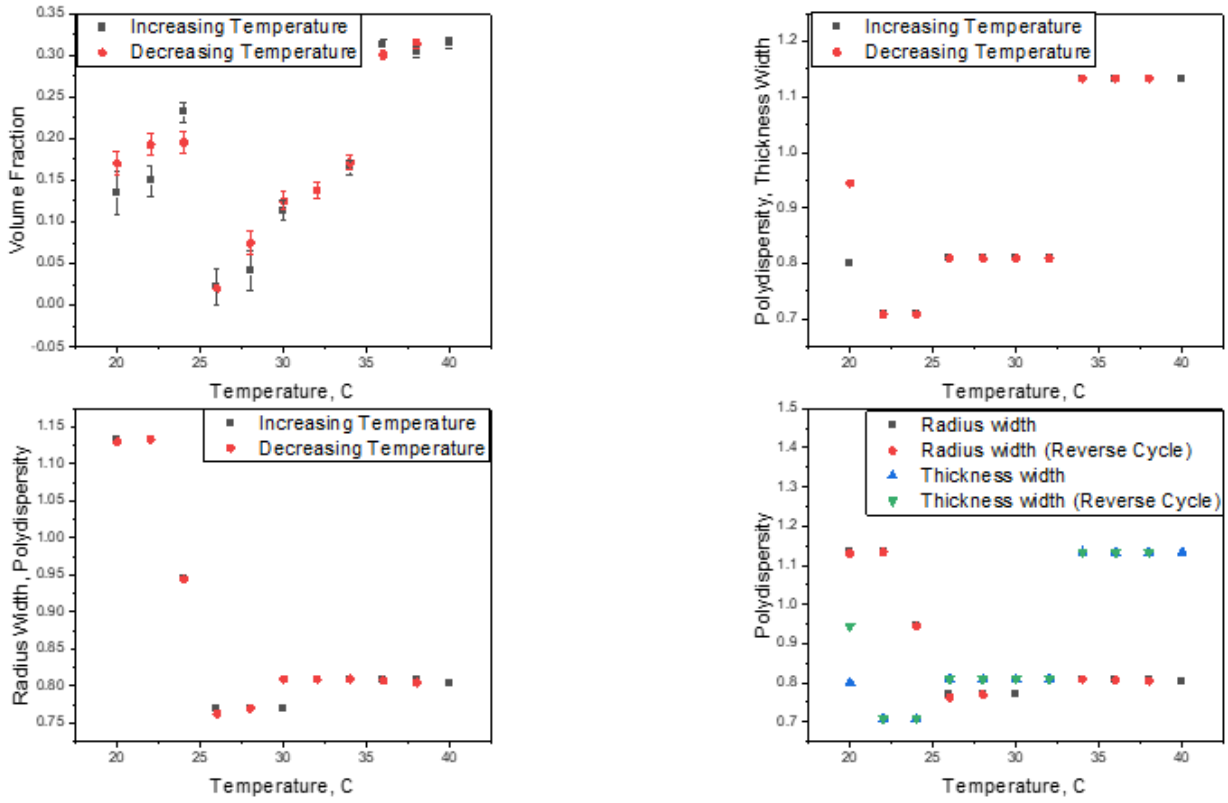

c d

Figure 20: Structural properties variation of 5% Pluronic F-127 at direct and reverse temperature variation where a) Volume fraction b) thickness width c) radius width and d) Comparison in radius width and thickness width

4.3.b) Pluronic F-127 Structural Properties Variation with Different Preparation Method

Pluronic F-127 has been prepared in two different methods. One preparation is done at room temperature and another at 60 0C. In this method, samples have been heated by a magnetic hot plate for an hour and then ultrasonicated with heat. Surprisingly, some structural properties are found different in both samples despite having the same composition. For example, the volume fraction increased from 0.15 to 0.75 with the change of temperature. In addition, the difference between the radius of core and thickness of shell for Pluronic F-127 also increased.

a b

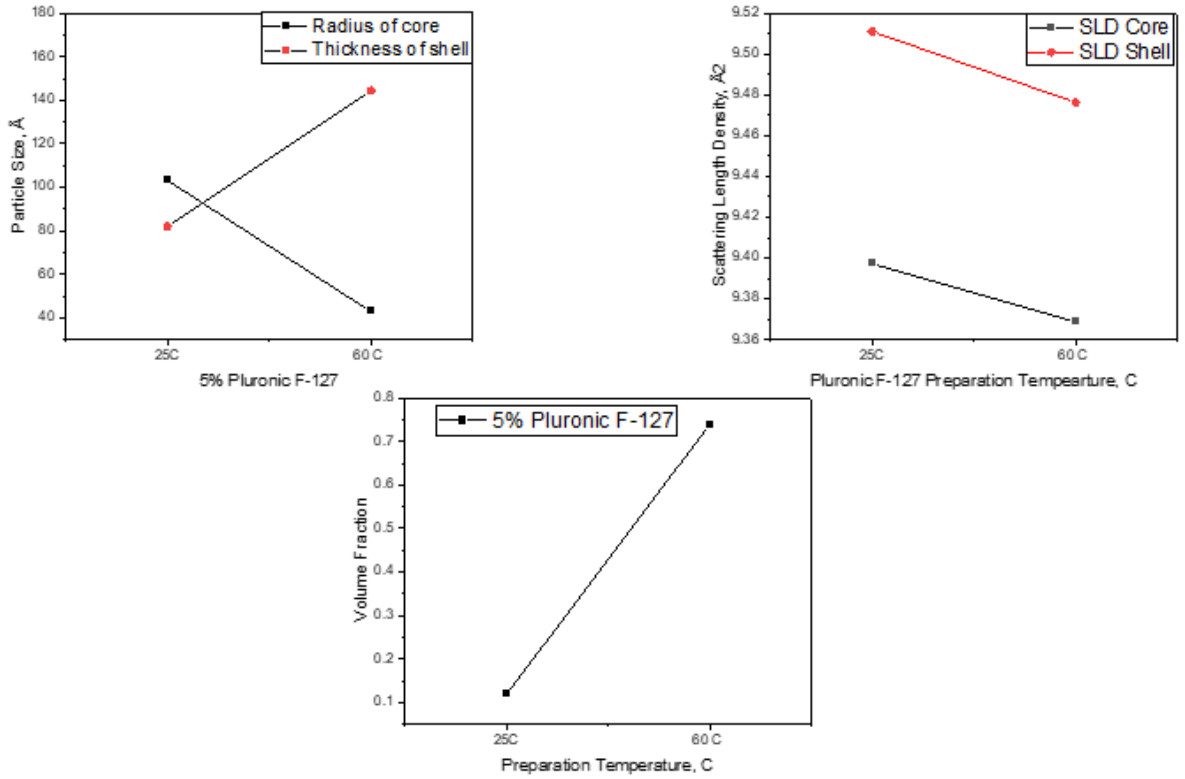

c

Figure 21: Structural properties variation in Pluronic F-127 micelles with different preparation method. Figure a) shows Particle size variation b) Scattering length density of core and shell c) Volume fraction of the particle.

After applying heat in preparation, the radius decreased, and thickness increased, whereas SLD values for core and shell decreased. Other than temperature variation, there can be several reasons for these discrepancies. The slightest disparity during raw sample weighing or time contrast between sample preparation and sample measurement might cause a significant difference. So, further analysis is required to be confirmed if different temperature introductions cause these inconsistencies during sample preparation. Nevertheless, according to the previous studies, different heating histories during sample preparation of Pluronic F-127 can give significantly different results because of the variation of domain sizes. An increment of temperature up to 50 0C can improve the ordered structure of micelles marginally. [37]

5. A) RESULTS FOR ALKANE LOADED PLURONIC F-127

5.1 a) Pluronic F-127 and Alkanes with Different Preparation Method

The scattering spectra are corrected after reducing background from electronic noise, sample holder, and buffer. Scattering intensity from two-dimensional raw data is reduced to one-dimensional scattering function. The plots shown below presents the scattering intensity I(q) of particles as a function of scattering vector q. Scattering vector can be expressed as,

$$q = \frac{4\pi}{\lambda} . \sin(\emptyset) \qquad (5)$$

Here λ I the wavelength of applied radiation and ∅ is known as azimuth angle.

After studying Pluronic F-127 micelles with different concentrations, Pluronic F-127 with 5%wt concentration has been chosen for further investigation. Pluronic F-127 with 5%wt concentration has been prepared along with 1%wt and 5%wt Hexane, respectively. After investigating the structural properties of Hexane at different concentrations, 5% wt concentration of alkane (Hexane, Octane, Decane, Dodecane) solutions have been prepared separately and with 5% Pluronic F-127 micelles. SAXS (Small Angle X-ray Scattering) measurement has been done on freshly prepared samples at room temperature. 5% Octane with 5% Pluronic F-127 sample showed very high intensity at low q region and seemed like Octane did not disperse nicely in the solution and did not let the micelle form. We will get clear about these data in the next section.

a b

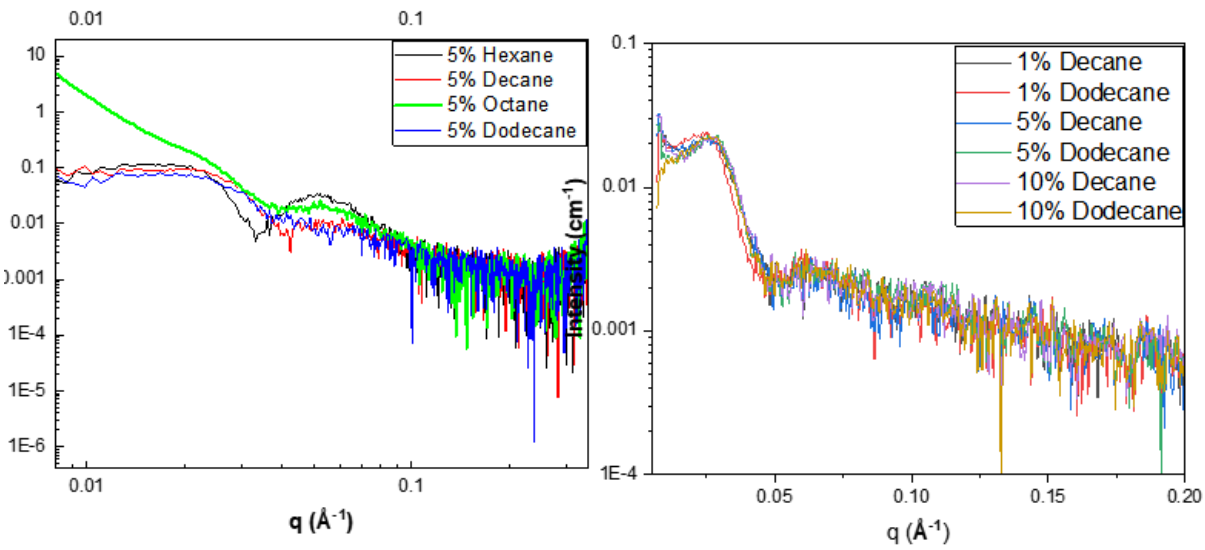

Figure 22: Alkane structure with 5% wt concentration of Pluronic F-127 a) 5% wt concentration of (Hexane, Octane, Decane, Dodecane) at room temperature b) 1%, 5% and 10% wt concentration of Decane and Dodecane prepared at 60 ^{0}C.

Further investigation has been found necessary on alkane and Pluronic F-127 solutions because of having opaque visibility in samples which indicates substantial aggregation in the particles; a change in preparation method was brought to get better homogenous and uniform solutions. 1%, 5%, and 10% wt concentration of Decane with 5% wt concentration of Pluronic F127 and 1%, 5%, 10% Dodecane with 5% Pluronic F127 have been prepared using magnetic stirring hot plate and analyzed using core-shell sphere model. First, samples have been heated using a magnetic stirring hot plate and then an ultrasonic bath. After applying ultrasonication and magnetic stirring, SAXS measurement was done at room temperature. Scattering intensity obtained from the reduced data of Decane and Dodecane showed similar plots, but further analysis is needed for understanding the parameters of different compositions.

5.2. a) Octane Loaded Pluronic F-127 micelles with Temperature Variation.

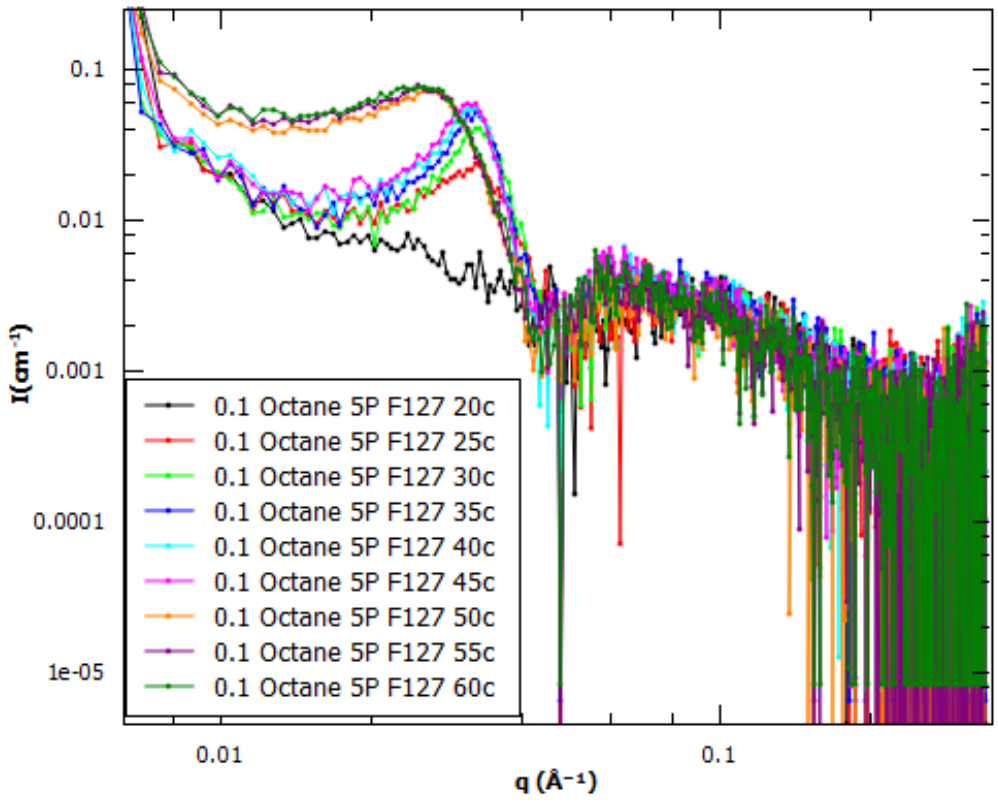

Figure 23: 5 % Pluronic F-127 scattering intensity variation with 0.1% Octane at different temperature

Figure 23 indicates the scattering intensity I(Q) of 5% Pluronic F-127 coupled with 0.1% Octane at several temperatures. Pluronic progresses from dissolved chains to micelles in a fluid-like order to micelle crystal structure with temperature alteration. All samples reveal a sequence of phase changes and signal of fluctuation in composition, which implies micellar formation in the solution. The increase in peak intensity due to phase change also indicates compositional contrast between exterior and interior of micelles, and intensity increases rapidly for more extended chain length

composition than short-chain length composition. [38] The peak shifted to left with a temperature increase, indicating the increment of inter micellar distance at higher temperatures.

5.B) DISCUSSIONS FOR ALKANE LOADED PLURONIC F-127

5.1.b) Structural Analysis of Alkane Loaded Pluronic F-127 at Room Temperature

Hydrocarbon solubilization greatly depends on the size and shape of surfactant micelles. Previously, it has been experimentally observed that long rodlike micelles have better solubility than small globular micelles. Also, rod to sphere shape transition concentration is higher with lower alkane chain length and microemulsion droplet size increases if CMC decreases which allows to form micelles. Rod like micelles becomes shorter and globular with increasing concentration of hydrocarbons. Size of swollen micelle also increases with increasing concentration of solubilizate (alkanes) and gains maximum size at the solubility limit. [39][40]

5% wt concentration of Alkanes (Hexane, Octane, Decane and Dodecane) have been prepared with 5% wt concentration of Pluronic F-127 micelles and their structural properties have been analyzed using SAXS. The core of micelle is hydrophobic, and shell has most of the hydrophilic portion.

The core of micelle is hydrophobic, and shell has most of the hydrophilic portion. The **Figure 24** (a) and (b) shows the radius of core and thickness of shell for each alkane with Pluronic F-127 solution. The graph shows, thickness of shell is larger than radius of core for all alkanes and core radius decreases with increasing alkane number. That indicates hydrophobic molecule concentration decreases at core of particle for higher alkane numbers. Also, most of the molecules spread out in the shell which causes the increase in shell thickness. Also, the charge of molecule discrepancy with increasing alkane number. The charge is similar for hexane, decane and dodecane

but much higher for Octane. Octane sample did not encapsulate inside micelles properly which caused the discrepancy in structural parameters.

a b

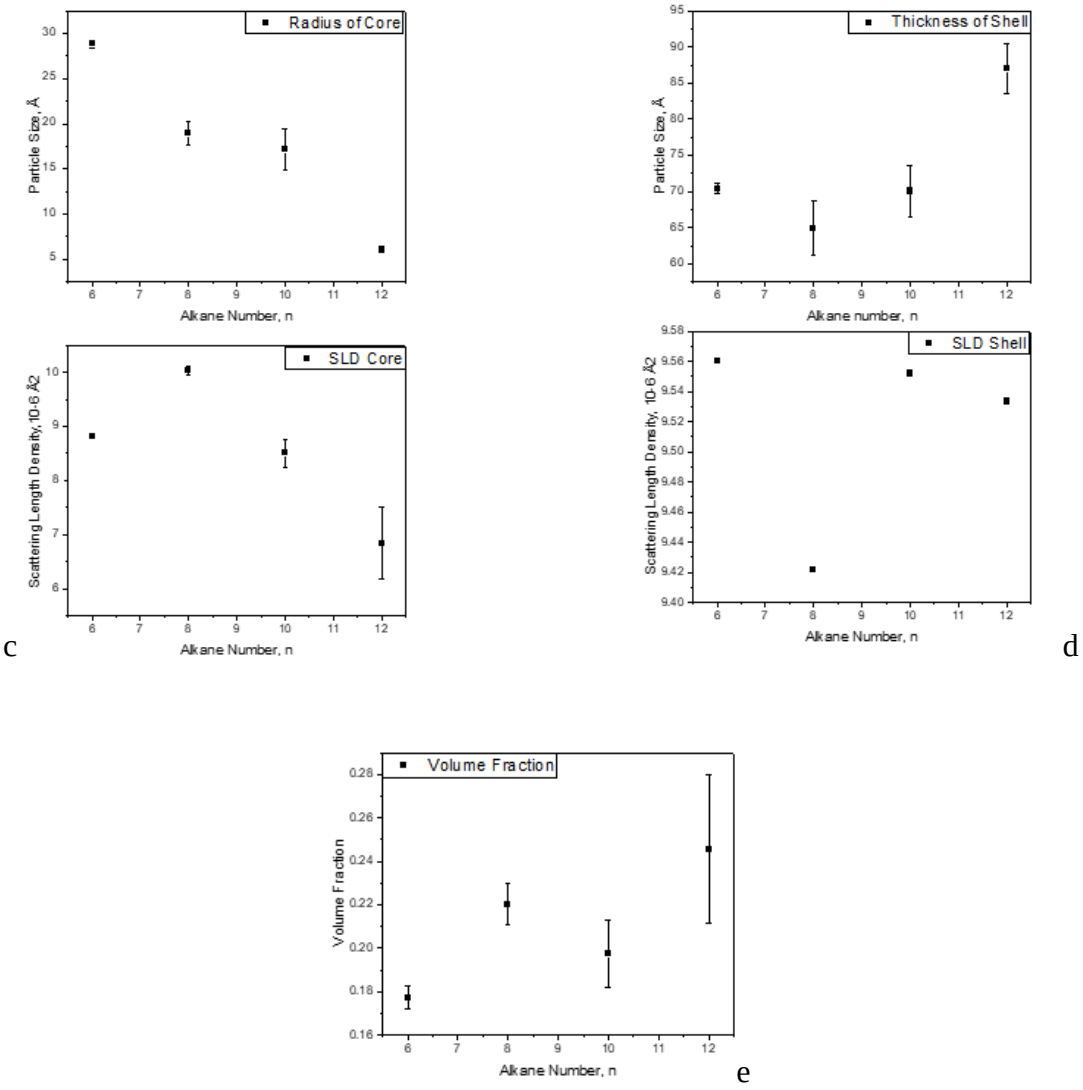

c d e

Figure 24: 5% Alkanes (Hexane, Octane, Decane, Dodecane) with 5% Pluronic F-127 at room temperature. (a) radius of core b) Thickness of shell c) SLD of core d) SLD of shell e) Volume fraction in alkanes of different alkanes prepared at room temperature.

.

Shows the radius of core and thickness of shell for each alkane with Pluronic F-127 solution. The graph shows that the thickness of the shell is more significant than the core radius for all alkanes. Core radius decreases, and thickness of shell increases with increasing alkane number. That indicates hydrophobic molecule concentration decreases at the core of particles for higher alkane numbers, and most of the molecules stay around the shell, which causes an increase in thickness. Let's compare **Figure 18** and **Figure 24. We** can see that the core of Pluronic F-127 micelles increased significantly after loading with alkanes, indicating the increase of core after encapsulating hydrophobic cargoes. This result aligns with the finding of a previous study. [21]

With increasing volume fraction value, the solubilization ability of the microemulsion phase reduces. [41] Plots convey a different nature of Octane solution, indicating a lack of micellar shape. As higher volume fraction causes poor solubility, Octane concentration might be too high to be encapsulated inside Pluronic F-127 micelles and intercepted the micelle formation. **Figure 24** (c) & (d) displayed the SLD of the core and shell of a sphere for different alkanes. SLD of the core is higher than shell for Hexane, Decane, and Dodecane. Apart from Octane, the SLD of core and shell decreased with increasing alkane number, and Dodecane has the lowest SLD value for core and shell.

Also, graph indicates the higher volume fraction for 5% octane with 5% Pluronic F-127 sample. Previous studies confirmed that the micelle charge increases with weight fraction and micelle volume decreases with increasing temperature, which agrees with the findings shown in **Figure 25** where the charge of samples increased with increasing concentration of Decane. [42]

5.2.b) Structural Analysis of Alkane Loaded Pluronic F-127 Prepared at High Temperature

Previously, Alkanes with Pluronic F-127 solutions have been mixed with magnetic stirring without applying any heat. Which might cause inhomogeneity among samples. To get consistent mixture, Decane and Dodecane have been prepared again using heat with different weight concentration 1%, 5% and 10%. **Figure 25** shows radius, thickness, and charge variation with respect to Decane and Dodecane concentration.

a b

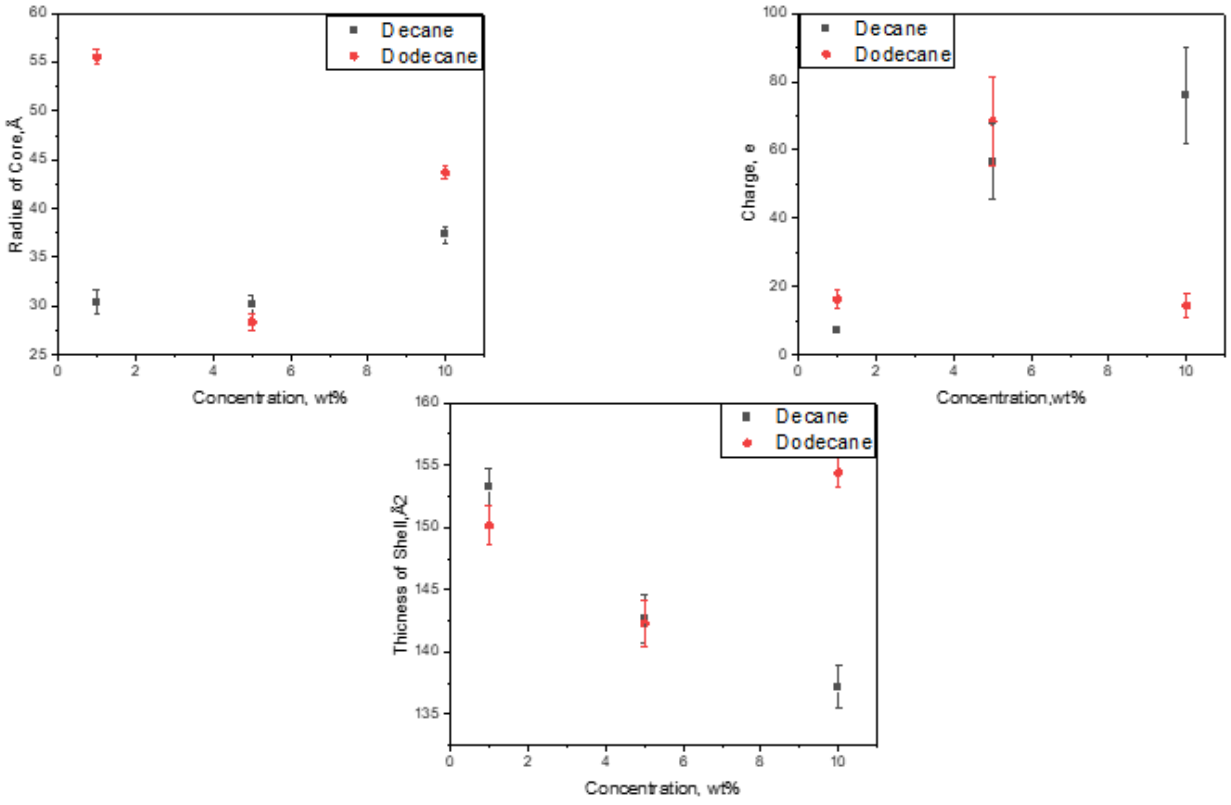

c

Figure 25: Different concentration of Decane and Dodecane loaded with Pluronic F-127 prepared at 60 ^{0}C. Where a) shows Radius of core b) Charge c) Thickness of Shell comparison between Decane and Dodecane.

The radius of core increases, and the thickness of the shell decreases with increasing Decane concentration, which indicates a hydrophobic molecule has increased in the core, which caused the increase in core size. The charge also increases with increasing Decane concentration. Knowing the charge of the molecule is essential because it keeps track of electrons and predicts reactivity. As charges and hydrophobic environments are naturally incompatible with each other, ions are usually excluded from the hydrophobic core and reside on the surface of a molecule, where it is more convenient to interact with water. Previous studies reveal that the dielectric constant of folded proteins is too low to prevent the needless existence of ions which causes destabilization of folded state and promotes aggregation. [43] So, a similar case can occur with hydrophobic molecules such as Pluronic F-127, alkanes, and fatty acids.

a

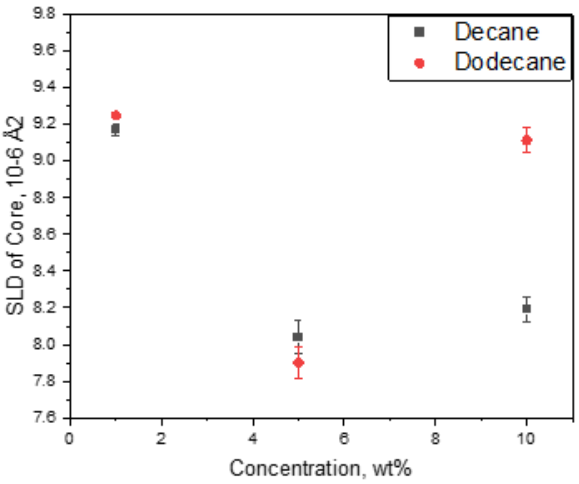

b

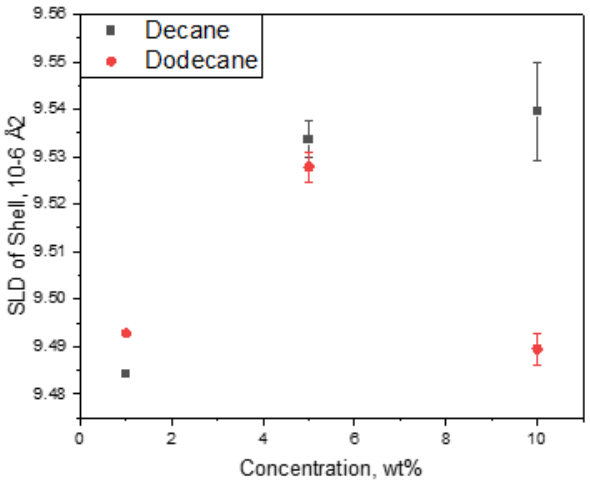

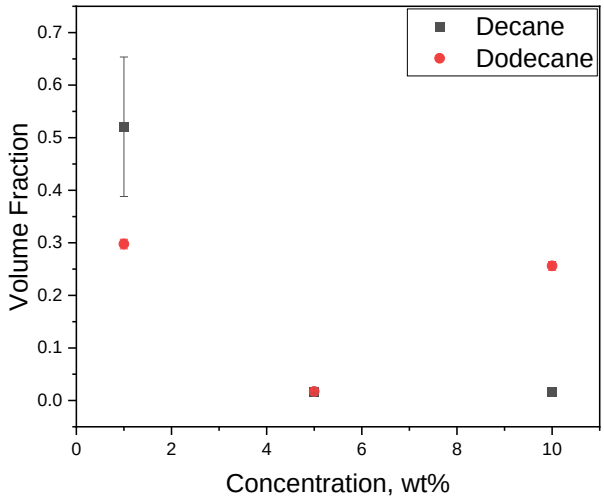

c

Figure 26 : Different concentration of Decane and Dodecane loaded with Pluronic F-127 prepared at 60 ^{0}C. Where a) and b) shows Scattering Length Density of core and shell c) volume fraction respectively of Decane and Dodecane.

Figure 25 shows that the core radius is much higher than the shell for all Dodecane and Pluronic F-127 samples. Shell thickness and radius of core decreased drastically at 5% Dodecane wt concentration but again increased at 10% wt concentration; for charge it varies oppositely. Pluronic F-127 concentration has been fixed at 5% for all compositions. **Figure 26** scattering length density of core is low for 5% Dodecane whereas SLD of shell is distinctly high from the other Dodecane samples. There might be a possibility that 10% Dodecane is not lying inside of micelles because of too much high concentration, and we see analysis of much less percentage of Dodecane sample than 10%. Further study is needed with narrow range of concentration to understand the discrepancy.

The density of polymer or surfactant molecule variation with distance can be expressed with volume fraction, which can provide information about surfactant or polymer molecules arrangement at the interface. The volume fraction is a ratio of volume of a component and total volume of the system, including the component. [44]

5.3.b Structural Analysis of Temperature Dependent Octane Coupled with Pluronic F-127

a b

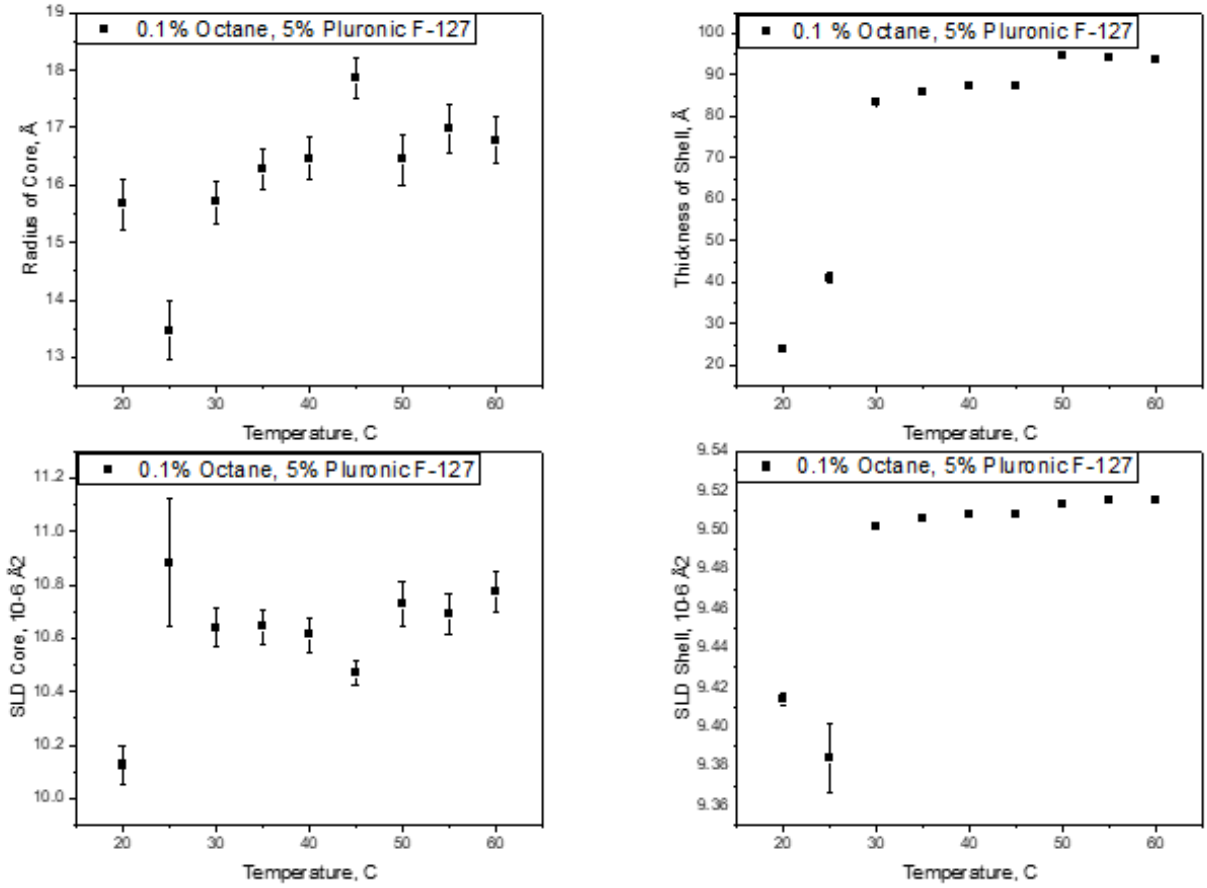

c d

Figure 27: Temperature dependent structural properties variation of 0.1% Octane and 5% Pluronic F-127 where a) shows radius of core b) Thickness of shell, Scattering Length Density of c) Core and d) Shell with respect to temperature.

a b

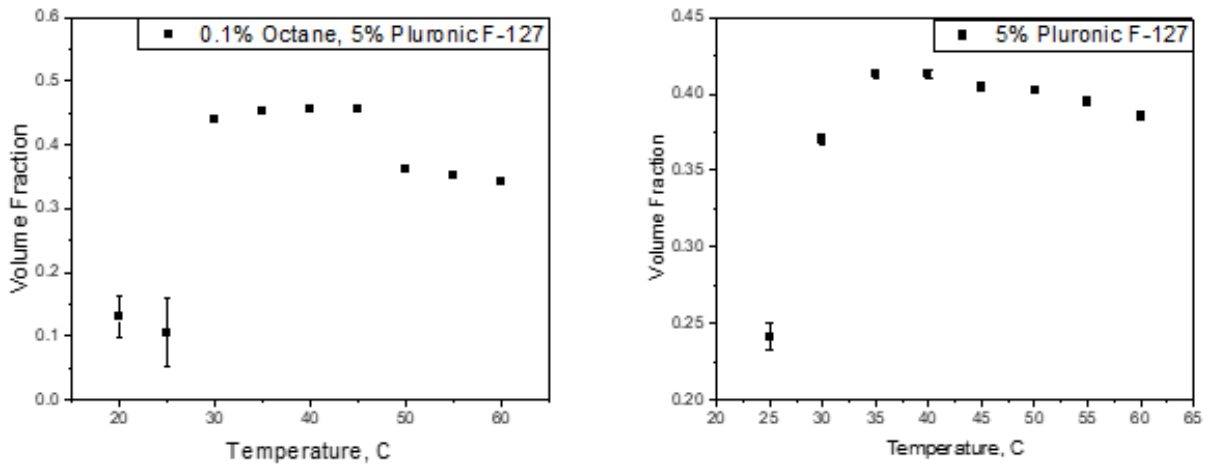

Figure 28: Temperature dependent volume fraction variation of a) 0.1% Octane and 5% Pluronic F-127 b) 5% Pluronic F-127

Figure 27 confirms the increment of radius of core and thickness of shell with increasing temperature. SLD or core and shell increased with temperature and two transitions have been observed in data. According to **Figure 28**, volume fraction remained almost constant between 30 ^{0}C to 45 ^{0}C. a transition has been observed in volume fraction and SLD core plots. If we take a closer look at all data from **Figure 27** and **Figure 28**, we will see a transition around 20-30 ^{0}C which occurred due to micelle formation and then sol-gel transition occurred around 40-45 ^{0}C. If we compare between the volume fraction of 5% Pluronic F-127 loaded with and without 0.1% Octane, smaller value for volume fraction around 20-30 ^{0}C can be noticed easily. As we know, micelle formation is not stable below CMT which might cause the reduction in volume fraction at low temperature. Volume fraction increases when temperature increases, and micelles are formed. After reaching the optimum environment for micelle formation, second transition occurs and volume fraction decreases. This might be caused because of sol-gel transition at higher temperature.

6. A) RESULTS FOR FATTY ACID LOADED PLURONIC F-127

6.1.a) Oleic acid with Pluronic F-127 Prepared at Room Temperature

2% and 10% Oleic acid have been prepared at room temperature with and without 5% Pluronic F-127 and scattering intensity has been measured as a function of scattering vector q. 2% and 10% Oleic acid does not show any micellar formulation because of the absence of Pluronic F-127.

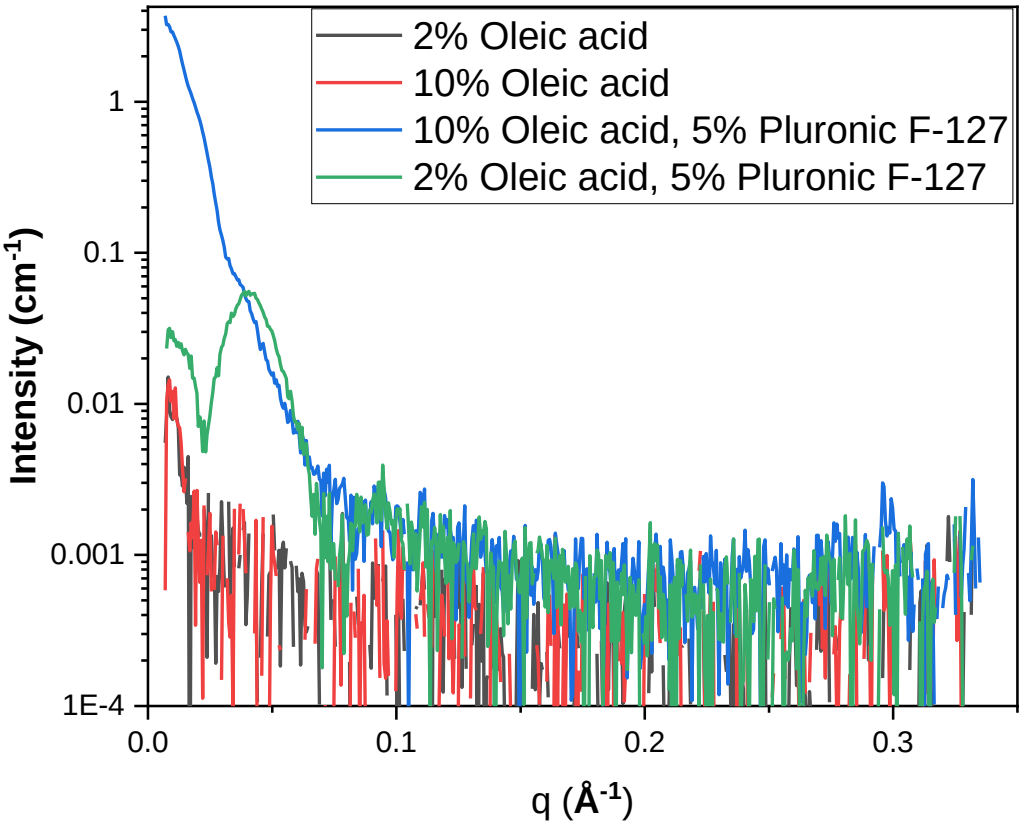

Figure 29: Different Concentration of Oleic acid with and without *5%* Pluronic F-127

Scattering intensity profile of 2% Oleic acid with 5% Pluronic F-127 showed micelle formation which indicates that Pluronic F-127 encapsulated the Oleic acid and formed micelles.10% Oleic acid with 5% Pluronic F-127 did not give sign of any micelle formation which might occur because

of over concentration of Oleic acid or inhomogeneous solution which did not let Pluronic F-127 to form micelles and encapsulate the hydrophobic cargoes. Further analysis is needed to understand the structure.

6.2.a) Linoleic acid with Pluronic F-127 Prepared at High Temperature

Sample of 2 wt% and 10 wt% linoleic acid, each with 5 wt% concentration of Pluronic F-127, and a 5% Pluronic F-127 reference sample were mixed using a magnetic stirring hot plate for 1 hour at 60 ° C, followed by ultrasonication at 60 0C or an hour. As linoleic acid and oleic acid are insoluble in water, it is tough to obtain 100% homogeneous dispersion at all parts of the SAXS sample cell. However, the final SAXS samples still had a visible difference in appearance. Thus each sample was measured at two different positions by SAXS to identify structural differences between the two distinct sample regions. The results have shown some interesting findings.

6.2.1 a) Linoleic acid and Oleic acid with Pluronic F-127

Figure 30 shows the comparison of scattering intensity among 2% ,10% Linoleic acid and Oleic acid loaded with 5% Pluronic F-127 and only Pluronic F-127 itself. All samples are prepared at 60 ^{0}C. 2% Linoleic acid and Oleic acid samples show sharp peak indicating micelle formation and peak intensity is higher than only Pluronic F-127 itself. The hump which indicates the micelle formation increased after adding cargoes, but 10% Linoleic acid seems to have too much concentration for encapsulating inside 5% Pluronic F-127. The structural properties of these fatty acids coupled with Pluronic F-127 will be discussed in later section.

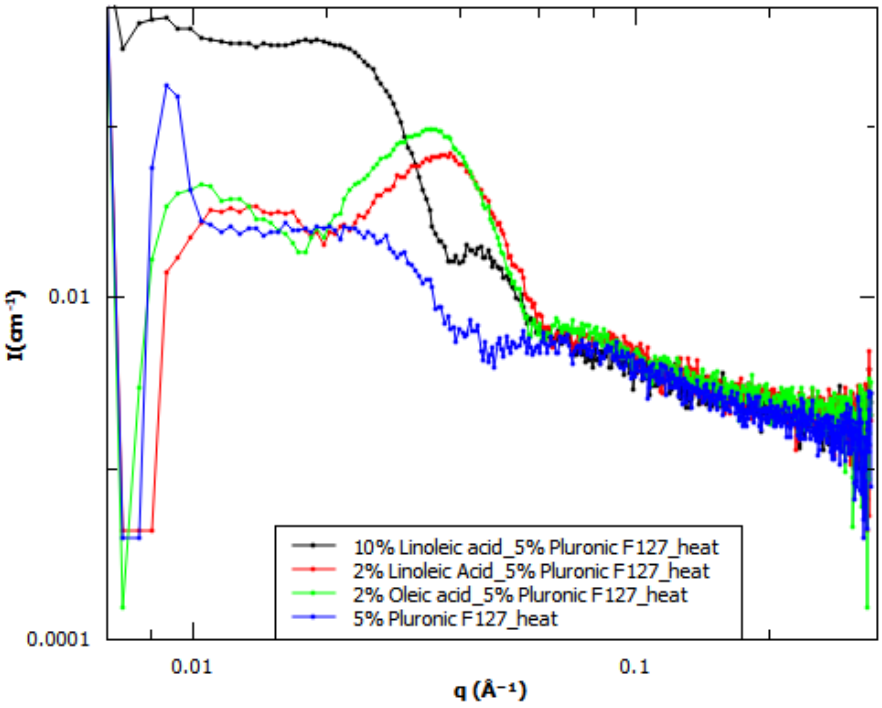

Figure 30: Linoleic acid and Oleic acid with Pluronic F-127 Prepared at 60 ^{0}C and Pluronic F-127 without cargoes.

6.2.2 a) Reduced Data of Linoleic Acid and Oleic acid Loaded with Pluronic F-127 at Different position

Figure 31 shows very different plots for the same samples at a different position. It is observed that for 2% Linoleic acid with 5% Pluronic F-127 no micellar nature has been observed at the bottom of the tube, but it is visible at the midpoint of the kapton tube. The firm peaks at q~0.04 indicate particle-particle solid interaction, which is expected in spatially ordered micelles. On the other hand, 10% Oleic acid with 5% Pluronic F-127 shows micelle formation. For Pluronic F-127 samples, plots are almost the same for both positions and show homogeneity.

a b

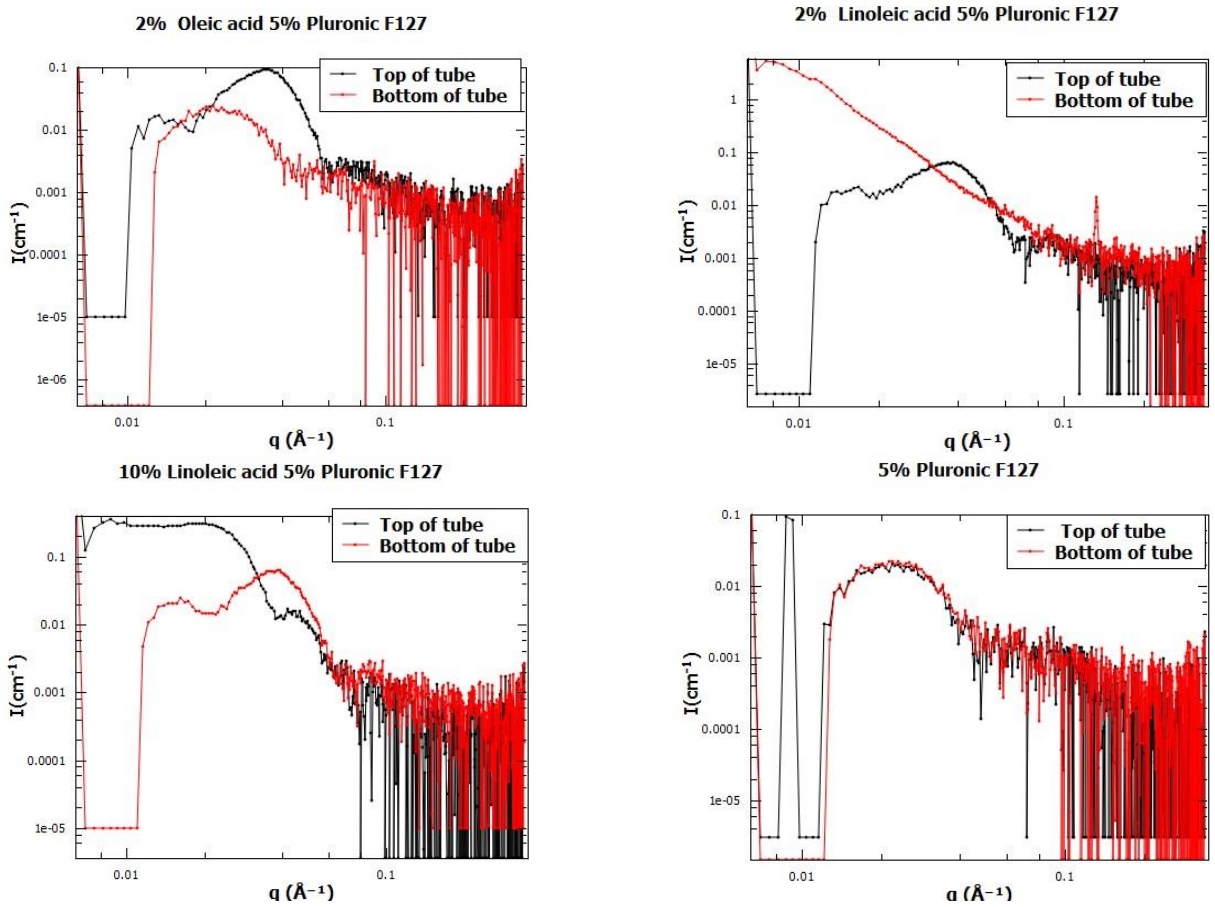

c d

Figure 31: Comparison at different positions of a) 2% Oleic acid with 5% Pluronic F-127 b) 2% Linoleic acid with 5% Pluronic F-127 c) 10% Linoleic acid with 5% Pluronic F-127 d) 5% Pluronic F-127

6.2.3.a) Low Concentration Linoleic Acid with Pluronic F-127 Characterization

Previously, Linoleic acid and Pluronic F-127 solutions have shown irregular patterns for different parameters which could be an indication of using too much Linoleic acid in 5% Pluronic F-127 micelle solution. Hence, very low weight concentration of Linoleic acid (0.05%, 0.1%, 0.2%) have been prepared with 5% wt concentration of Pluronic F-127. From reduced data plot, transition of nature is observable from 0.05% to 0.2% wt concentration of Linoleic acid.

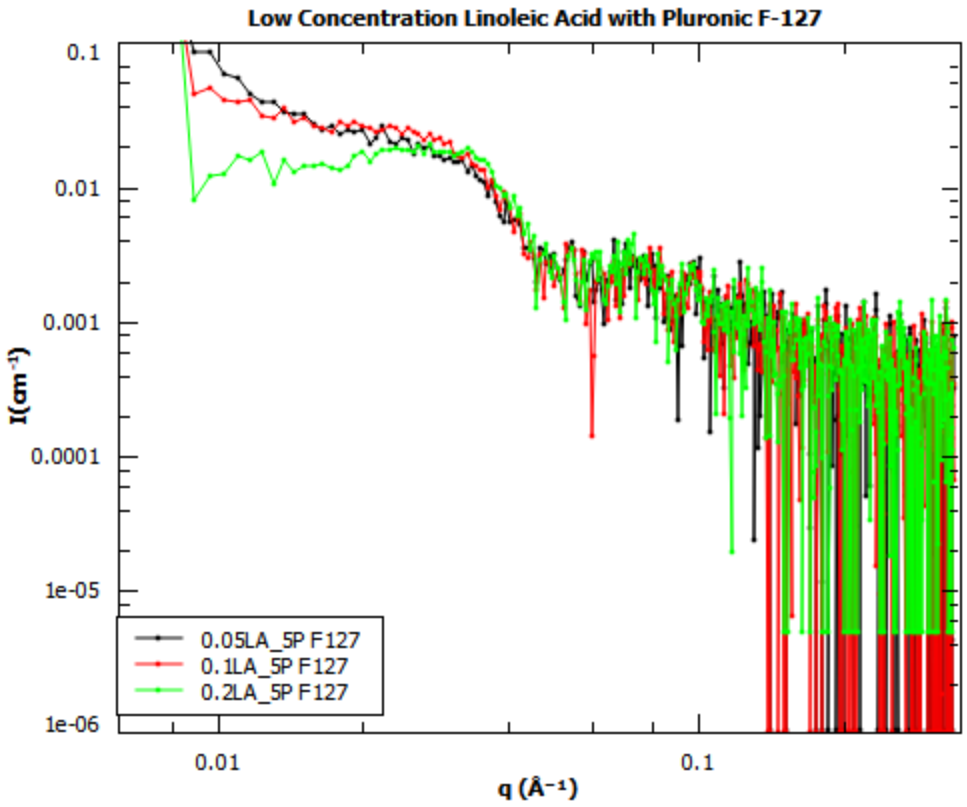

Figure 32: Data Pattern of different weight concentrated (0.05%, 0.1%, 0.2%) Linoleic acid coupled with 5% Pluronic F-127

6.2.4.a) Temperature Variation of Linoleic Acid Coupled with Pluronic F-127

Scattering spectrum of 0.1% Linoleic acid associated with 5% Pluronic F-127 have been observed at different temperature. Temperature has been varied from 20 to 60 ^{0}C with 5 ^{0}C temperature increment in every 30 minutes. **Figure 33** shows micellar formation at all temperature but peak intensity increases with increasing temperature. With the increase of temperature and concentration, copolymer chains form spherical micelles initially. Peak shifted toward left which conveys that inter micellar distance is increasing with temperature. Core can be expressed using hard sphere form factor and shell/corona can be expressed using Gaussian coil form factor. [35]

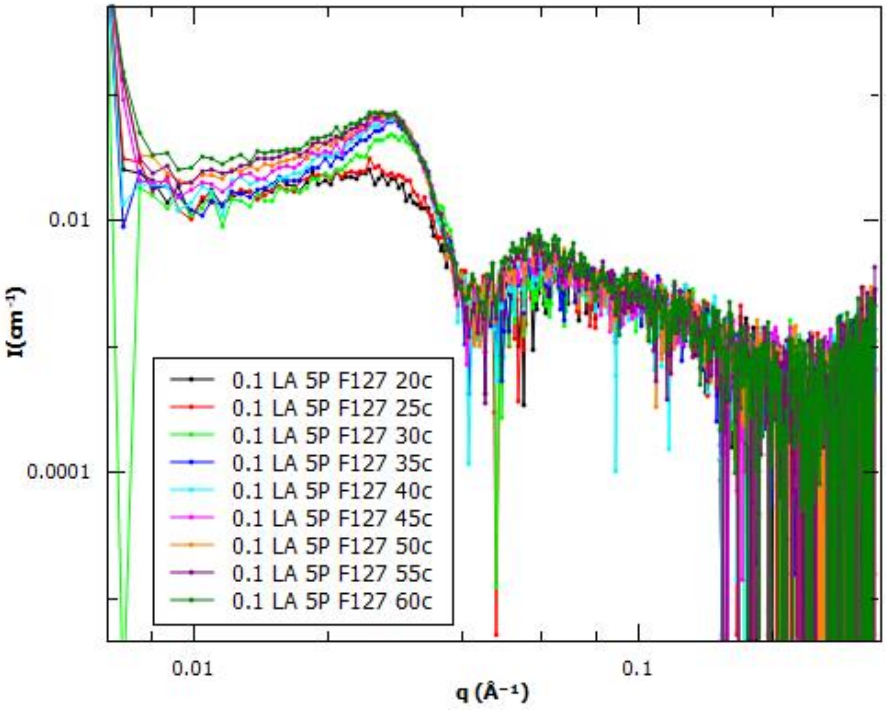

Figure 33: 0.1% Linoleic acid with 5% Pluronic F-127 at temperature variation from 20 ^{0}C to 60 ^{0}C

6.B) DISCUSSIONS ON STRUCTURAL PROPERTIES OF OLEIC ACID AND LINOLEIC ACID LOADED WITH PLURONIC F-127

6.1 b) Oleic Acid Prepared at Room Temperature

Pluronic F-127 micelles with 5% wt concentration has been analyzed with 2%, 10% Oleic acid and 2.5% of Pluronic F-127 has been analyzed with 1% and 5% Oleic acid. These two pairs of composition have same ratio of micelle and cargo, but the water amount is different. 1% Oleic acid with 2.5% Pluronic F-127 and 2% Oleic acid with 5% Pluronic F-127 has comparable structural parameters which makes sense because these samples have same component ratio. Surprisingly, radius and thickness at 5% Oleic acid with 2.5% Pluronic F-127 and 10% Oleic acid with 5% Pluronic F-127 are distinctly different despite having same ratio in the solution. In **Figure 34**, very low radius of core and thickness of shell have been observed for 10% Oleic acid samples comparing to other compositions. Also, SLD for core-shell and charge are very high for 10% Oleic acid composition. These disparities might occur because of the presence of different amount of solvent or preparing samples without applying any heat. As samples were not heated during mixing, mixture might not be uniform so further investigation is needed to examine the difference in structure with and without heating. Also, the concentration of 10% Oleic acid might be too much for acting as a cargo of micelle. But 2.5% Pluronic F-127 samples followed a pattern, radius of core decreased, and thickness of shell increased with increasing Oleic acid concentration. Oleic acid has carboxylic acid in the chain which attracts water and results in increase of thickness. At higher concentration, water gets removed from the core and core size decreases.

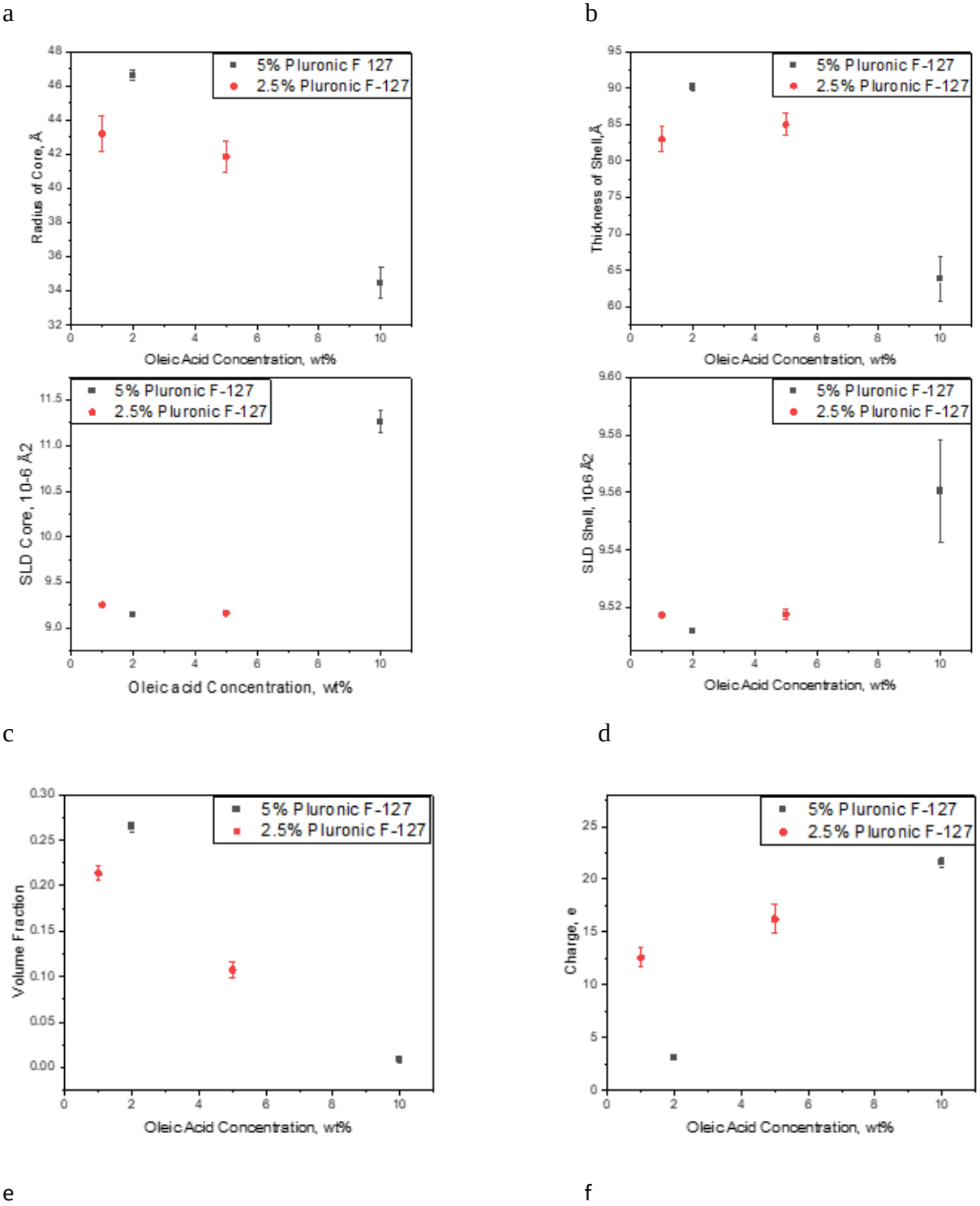

Figure 34: Structural parameter comparison among Oleic acid (1%, 2%, 5%, 10%) with 2.5% and 5% Pluronic F-127 where a) Radius of core b) Thickness of shell, c) SLD of core d) SLD of shell e) Volume Fraction f) Charge

6.2 (b) Comparison between Oleic Acid with Pluronic F-127 Prepared with Different Method

Figure 35 displays lucid dissimilarity between 10% and 2% Oleic acid with 5% Pluronic F-127 prepared using temperature induced method. 10% Oleic acid with F127 graph obtained from Figure 29 indicates that there might not have any micelle formed in that composition. This may happen because 10% Oleic acid has an unconventional weight concentration for Pluronic F-127 micelles. Radius and thickness of Oleic acid compositions prepared at 25 ^{0}C and 60 ^{0}C have been investigated to get a clear idea about the situation. For samples prepared at room temperature, Radius of core and thickness of shell decreased with concentration. But for samples prepared at 60 ^{0}C, radius of core increased, and thickness of shell decreased with temperature.

a b

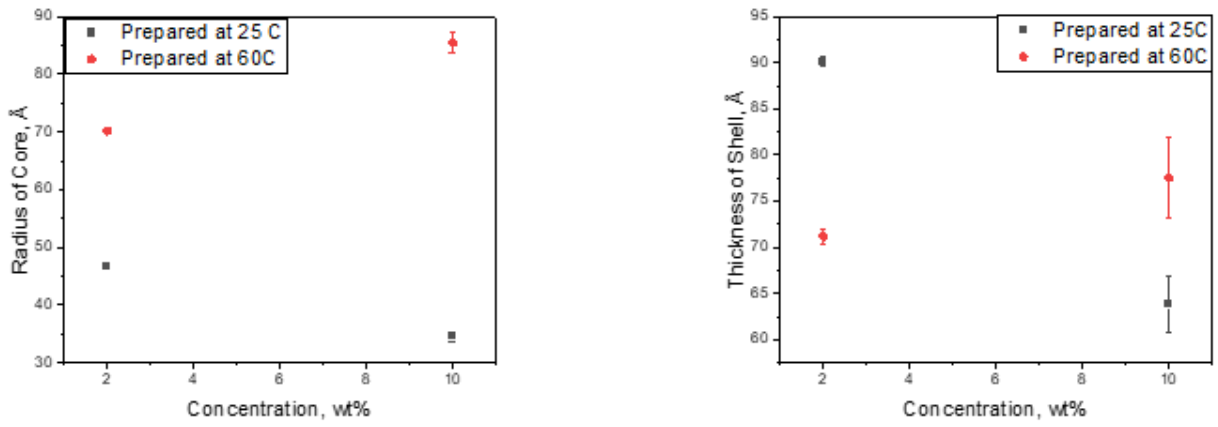

Figure 35: Comparison of a) Radius of Core b) Thickness of shell among Oleic acid prepared at different temperature.

After temperature treatment, samples with same composition have been measured by SAXS again. Thickness of shell increased in samples of higher concentration loaded with 5% Pluronic F-127

which follows the same pattern as 2.5% Pluronic F-127 samples. At higher concentration thickness of shell increased as we have seen in 1% and 5% Oleic acid with 2.5% Pluronic F-127 samples.

6.3.b) Structural Analysis of Linoleic Acid Loaded with Pluronic F-127 Prepared at High Temperature

a b

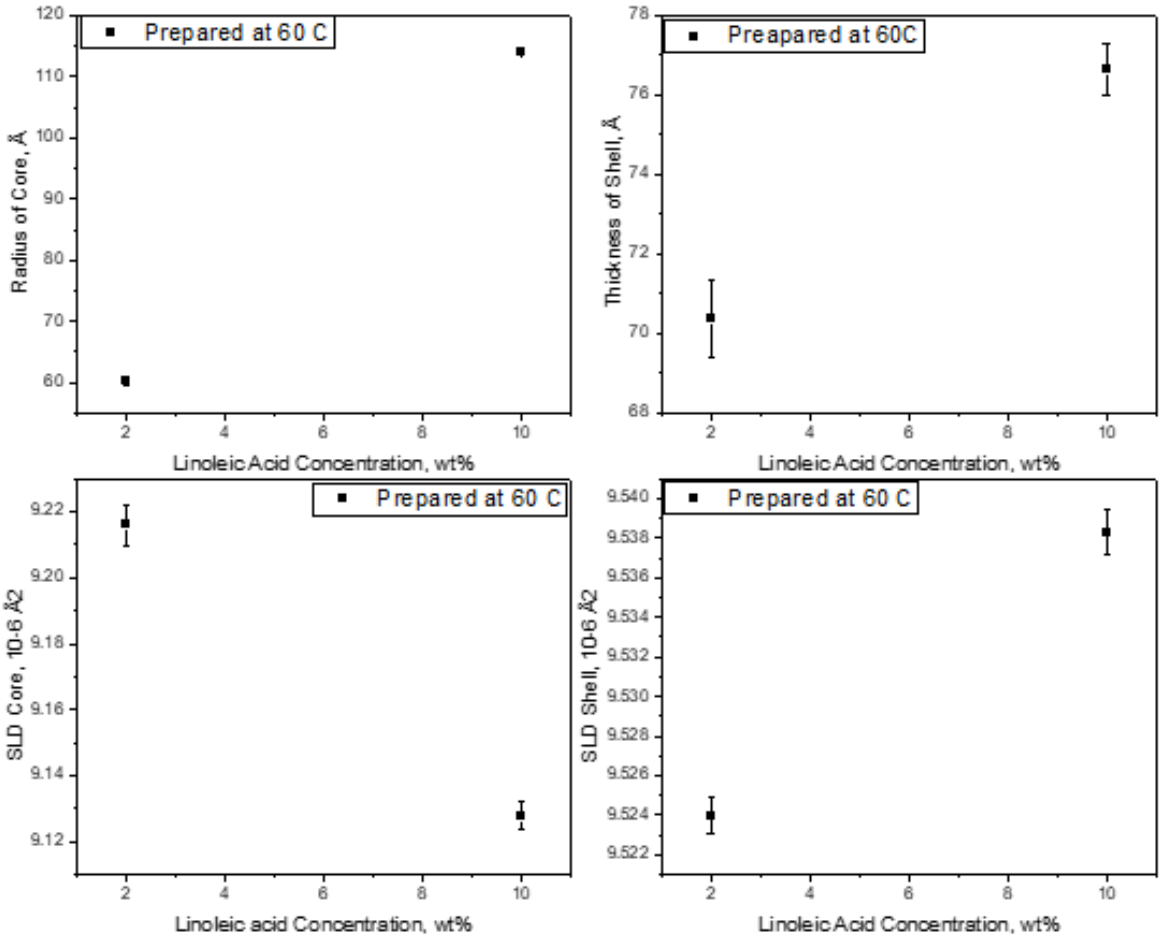

c d

Figure 36: Different Concentration (2%, 10%) of Linoleic acid with 5% Pluronic F-127 Prepared at 60 ^{0}C where a) shows radius of core b) Thickness of shell c) SLD of core d) SLD of shell.

Figure 36 displays the change of radius of core, thickness of shell, SLD core and SLD shell of 2% and 10% Linoleic acid loaded with 5% Pluronic F-127. Radius of core and scattering length density

of core decreased with increasing Linoleic acid concentration. Also, thickness of shell and SLD of shell increased with increasing Linoleic acid concentration. This indicates less electron density and reduction of hydrophobic cargoes inside the core after increasing Linoleic acid concentration. If we compare these values with 5% Pluronic F-127 results shown in **Figure 18** we can see the increase of radius and thickness after coupling Pluronic F-127 with Linoleic acid.

6.4.b) Oleic Acid and Linoleic Acid Comparison Prepared at High Temperature

Yuki et al. studied the epoxidation rate for Oleic acid and Linoleic acid, and he found reaction rate is higher for Oleic acid because of having lower number of C=C double bonds. Also, better optimized condition has been availed by using Pluronic conjugate as enzyme catalyst with fatty acids. [45]

Figure 37 compares 2%, 10% Oleic acid, and Linoleic acid with 5% Pluronic F-127. The thickness of the shell for 2% Oleic acid and 2% Linoleic acid is almost the same. Similar results have been found for 10% Oleic acid and 10% Linoleic acid where the thickness of the shell is next to same. But radius and charge of Oleic acid and Linoleic acid in different concentrations convey otherwise.

Comparison among the scattering length density, volume fraction and charge properties of Oleic acid and Linoleic acid at different weight concentrations are also shown. SLD of core for 2% samples is also alike, but the value is much higher for 10% Linoleic acid than 10% Oleic acid solutions. This result disposes of the possibility of higher electron density in core of 10% Linoleic acid with 5% Pluronic F-127 than 10% Oleic acid with 5% Pluronic F-127. Also, according to **Figure 37 (c)** the charge of 10% Linoleic acid solution is more significant than that weight percentage of Oleic acid. Plots manifests, the volume fraction of particles decreased with increasing weight concentration of fatty acids (Oleic acid, Linoleic acid). Also, values for both

fatty acids are comparable, and for both cases, there is high possibility that 10% of fatty acid is not present inside the micelles, rather dispersed over the whole solution.

a

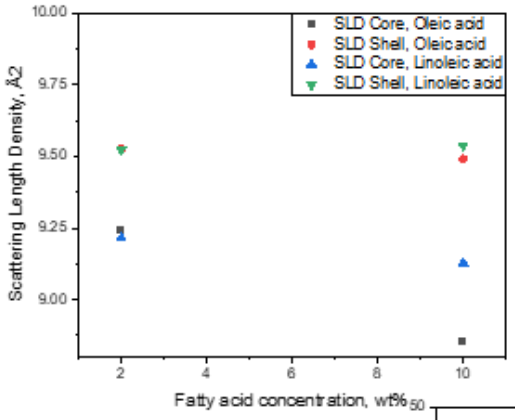

b

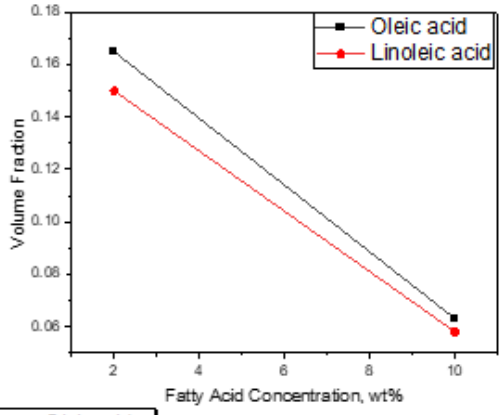

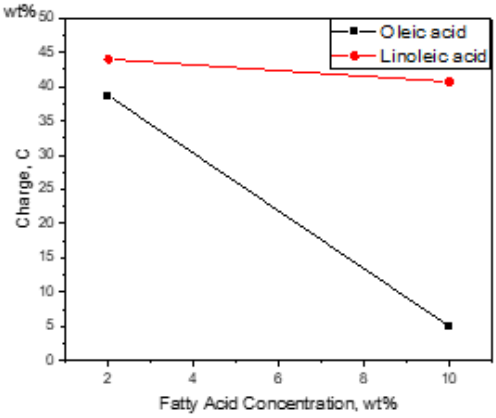

c

Figure 37: Comparison of a) Scattering Length Density b) Volume fraction c) Charge of Oleic acid (2%,10%) and Linoleic acid (2%, 10%)

6.5.b) Low Concentration Linoleic Acid with Pluronic F-127

6.5.1 (b) Core Shell Sphere Fitting on Low Concentration Linoleic Acid with Pluronic F-127

a b

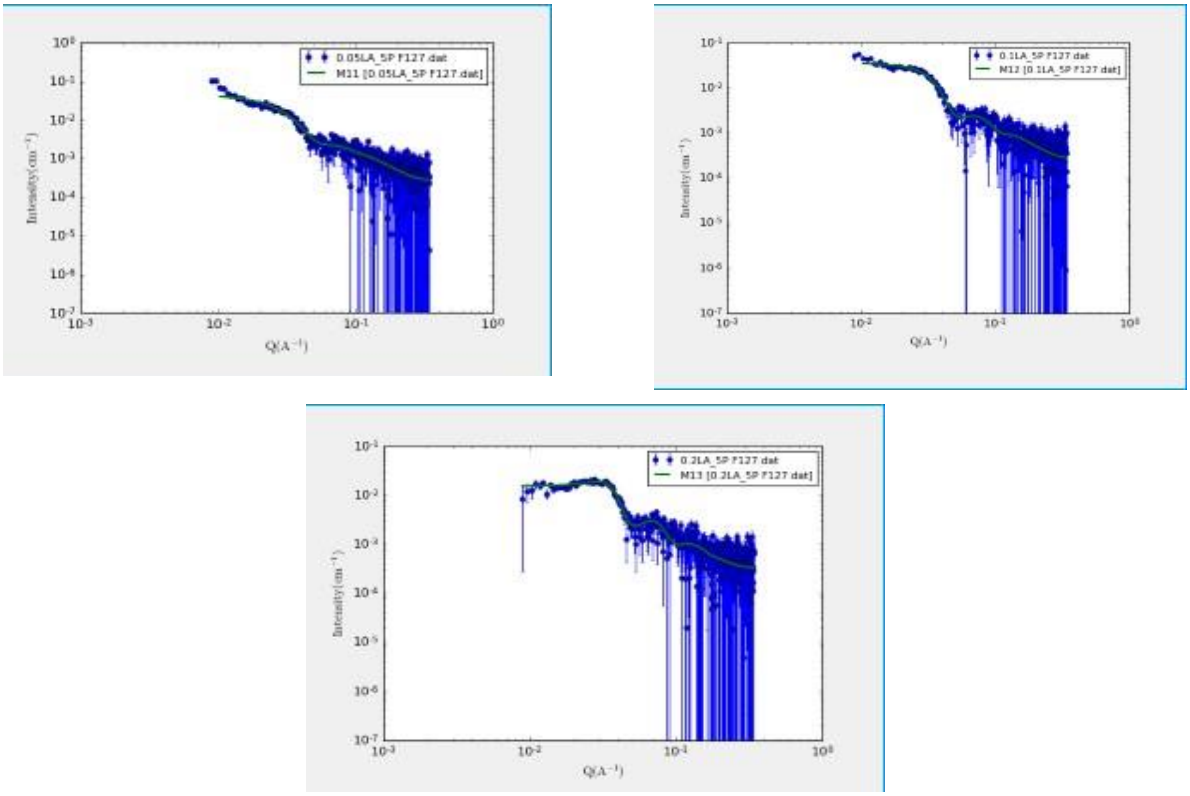

c

Figure 38 : Core shell sphere with hard sphere model fitting on different weight concentration of Linoleic acid (a) 0.05% Linoleic acid (b) 0.1% Linoleic acid (c) 0.2% Linoleic acid with 5% Pluronic F-127 micelles

Figure 38 shows the increment of hump in the samples with increase of Linoleic acid concentration. The hump indicates the micellar interaction which is visibly clear in 0.2% Linoleic acid with 5% Pluronic F-127.

6.5.2.b) Structural Analysis of Low Concentration Linoleic Acid with Pluronic F-127

So far this study has shown a detailed discussion on structural properties for different alkanes, fatty acids and drug with different weight concentration prepared with different method. Some samples showed a pattern and some didn't follow any pattern. So, this work has need of investigating the properties in much lower concentration. With the aim of getting a lucid idea about the properties, structures have been analyzed for 0.05%, 0.1% and 0.2% Linoleic acid along with 5% Pluronic F-127.

a

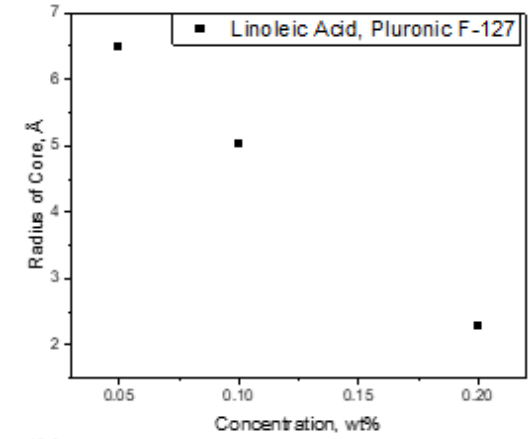

b

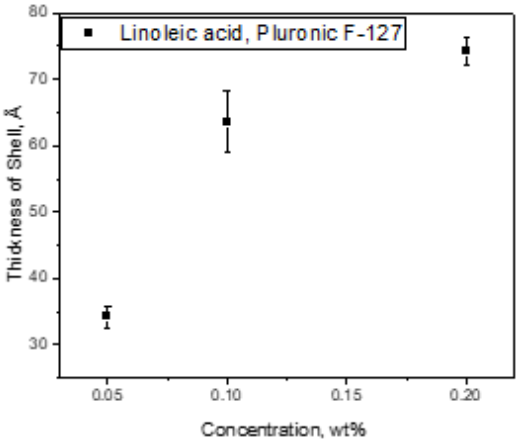

c

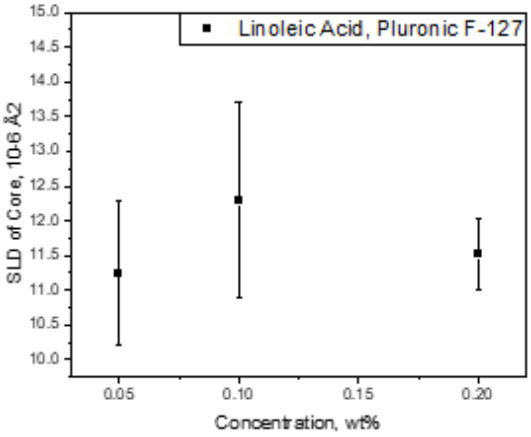

d

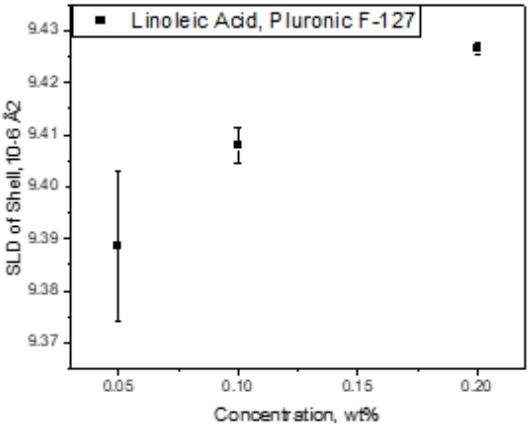

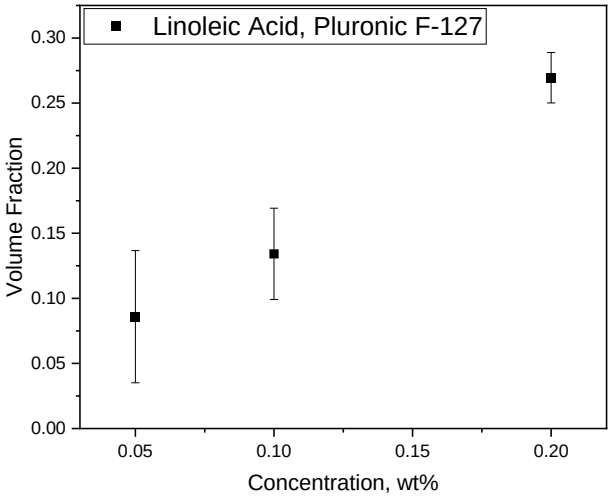

e

Figure 39: Structural parameters of Linoleic acid (0.05%, 0.1%, 0.2%) with 5% Pluronic F-127 where a) Radius of Particle b) Thickness of shell c) SLD of core d) SLD of shell e) Volume fraction

Figure 39 indicates that radius of core decreased, thickness and SLD of shell incresed with higher Linoleic acid concentration. Also, volume fraction increased with increasing Linoleic acid weight concentration. As we can see, thickness and SLD of shell increased with concentration which conveys the increased presence of Linoleic acid in the shell.

Conjugated linoleic acid (CLA) is considered a chemo preventive agent that enhances anticancer efficacy if coupled with Pluronic F-127 micelles. CLA has limitations in clinical application due to low solubility in water. An efficient drug delivery system can be obtained by the attachment of low molecular weight anticancer agents and micelles.[46] Moreover, Linoleic acid's low water solubility can be helpful to encapsulation into the hydrophobic core of micelles.

0.1% of Linoleic acid with 5% Pluronic F-127 structure has been analyzed with temperature variation and then compared with 5% Pluronic F-127 sample. **Figure 40** indicates a phase transition around 30-40 ^{0}C, and we can see an increase in radius of core, thickness of shell and

SLD of core after phase transition. We can also see a transition around 25 ^{0}C due to micelle formation. Radius and SLD of core increased, thickness decreased after addition of Linoleic acid in Pluronic F 127. However, SLD shell remained almost constant and held the same value as the Pluronic F-127 sample. This indicates the electron density of the shell did not affect much after coupling with Linoleic acid.

a b

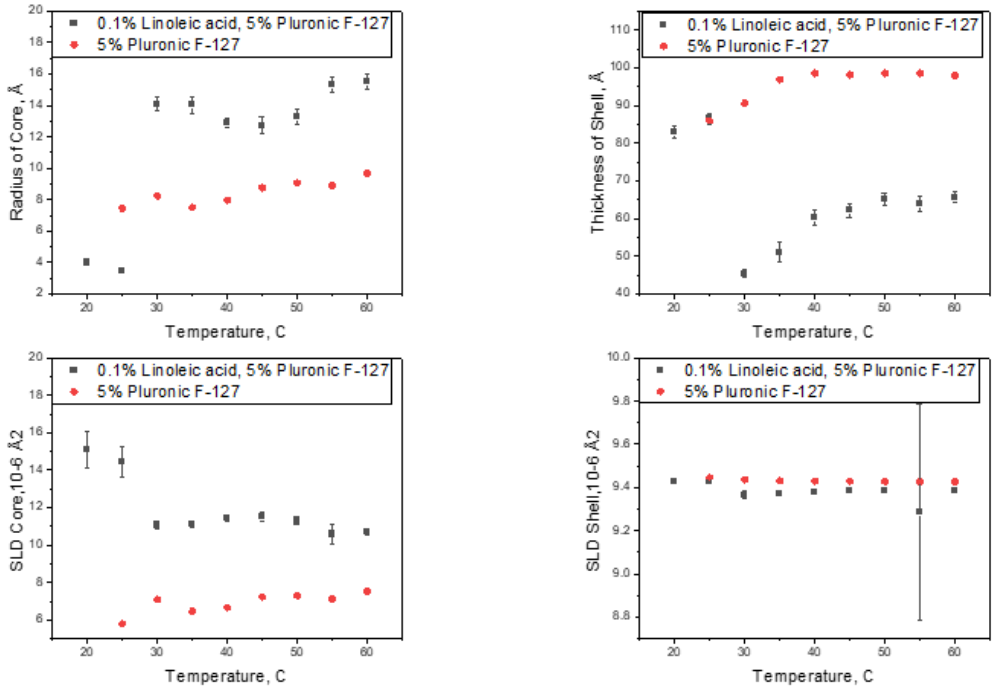

c d

Figure 40 : Temperature dependent structural properties variation of 0.1% Linoleic acid and 5% Pluronic F-127 where a) shows particle size b) Scattering length density variation of core and shell and c) Volume fraction of particle d) Charge variation with respect to temperature.

Figure 41 displays the volume fraction of 0.1% Linoleic acid with 5% Pluronic F-127 and 5% Pluronic F-127 without cargoes. It shows that volume fraction decreased after the addition of Linoleic acid and the charge decreases gradually after phase transition around 20-30 ^{0}C. According to these analyses, volume fraction values are close to zero, and core sizes are very tiny.This

indicates that Linoleic acid contributes to form the shell, and the hydrophobic molecule is not reliable inside micelles.

a b

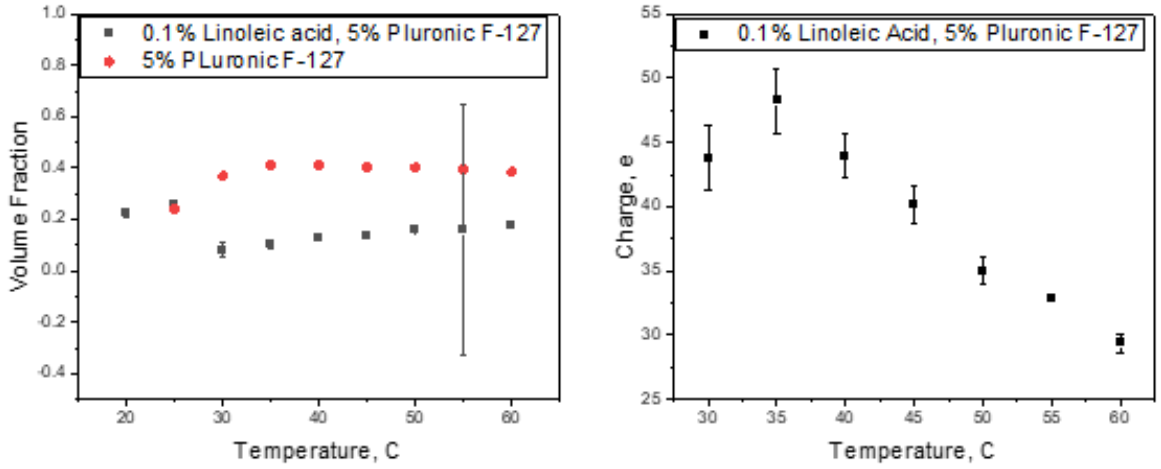

Figure 41: Temperature dependent structural properties variation of 0.1% Linoleic acid and 5% Pluronic F-127 where a) shows volume fraction b) charge variation.

6.6.b) Temperature Dependent pH Comparison of Low Concentration Linoleic Acid with Pluronic F-127

pH of sample can play a vital role in controlling hydrophobicity, which makes the need of investigating pH variation among the hydrophobic molecules crucial. Previous studies show, low pH triggers the increase in hydrophobicity in Collicin E3 which is type of plasmid-encoded bactericidal protein.[47] For this study, pH of Linoleic acid at very low concentration (0.05%, 0.1% and 0.2%) associated with 5% Pluronic F-127 micelles have been investigated with the temperature variation. To understand the pH imbalance more accurately, pH meter has been calibrated and pH values have been observed both with increasing and decreasing temperature.

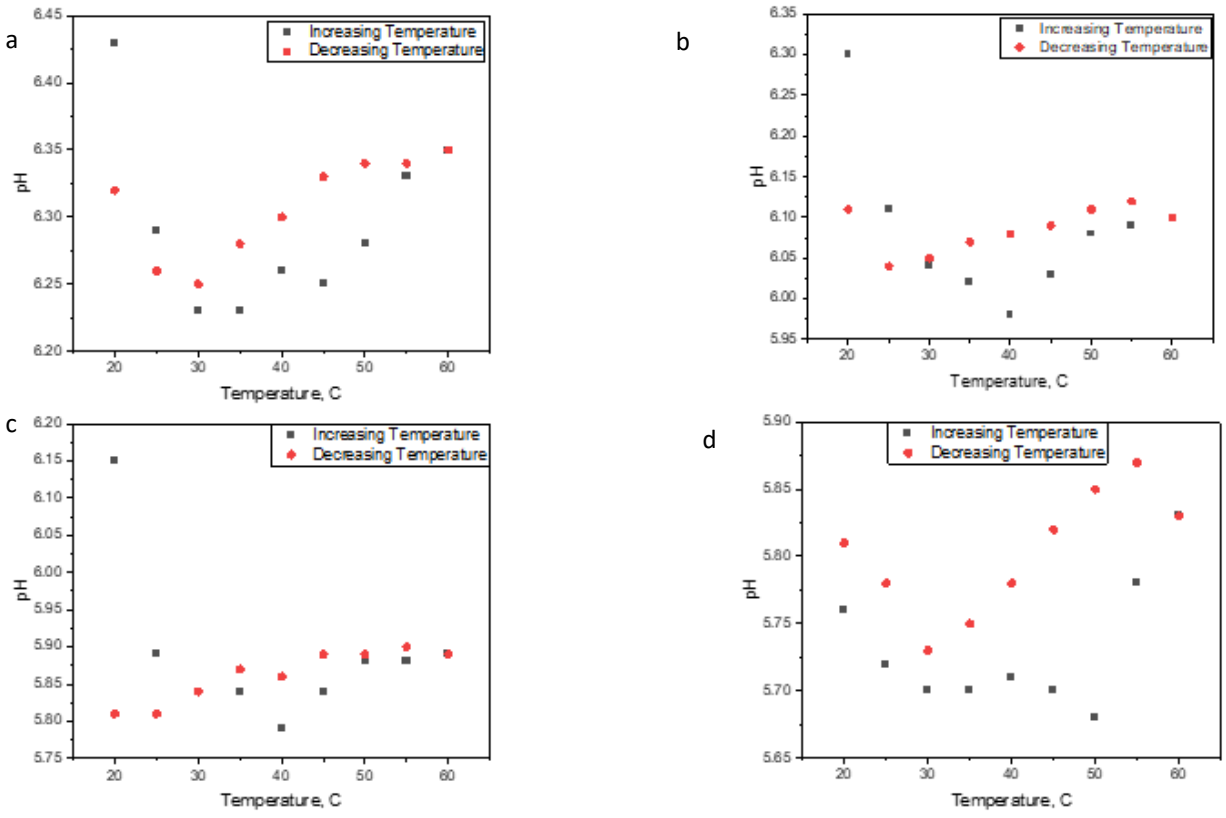

Figure 42: pH and Temperature Comparison of Low Concentrated Linoleic acid with Pluronic F-127 (a) 0.05% Linoleic acid with 5% Pluronic F-127 (b) 0.1% Linoleic acid with 5% Pluronic F-127 (c) 0.2% Linoleic acid with 5% Pluronic F-127 (d) MilliQ water

Usually, molecular vibration increases at higher temperature which escalate the ionization and causes pH drop. Also, change of micellar structure can be a reason of pH drop as well. In **Figure 40**, we have seen the expansion of the shell of Linoleic acid sample around 40 ^{0}C. An irregularity in pH values at different temperature might not be an error, it simply indicates the accurate pH value at that temperature. Composition of mixture is also important along with temperature and pH can be independent of temperature for some composition. Cecilia et al. studied, effects of temperature on pK_a can be larger for amines, phenol and pyridine where benzoic acid is independent on temperature variation. [48]

Figure 42 shows pH comparison with temperature for lower concentration of Linoleic acid (0.05%, 0.1%, 0.2%) with 5% Pluronic F-127 micelles. Also, pH of ultrapure milliQ water has been observed with temperature variation. From this experiment, pH decreases with increasing weight concentration of Linoleic acid. Also, pH value for a specific temperature has been found very similar during increment and decrement of temperature. During measuring pH of these samples, pH probe was injected inside the water of the ultrasonic bath during the whole experiment. This might be a reason of having better control over the pH variation with temperature.

If we compare **Figure 41** and **Figure 42**, pH increases slowly from 40 ^{0}C to 60 ^{0}C and the charge decreases slowly with the increase of temperature. From previous studies, we know the isoelectric point (PI) of Pluronic F-127 is around 5.00, which is less than the pH we have observed in our Linoleic acid-loaded Pluronic F-127 samples. As PI<pH, micelles already have a negative net charge during measurement.[8] For 0.1% Linoleic acid with 5% Pluronic F-127, pH increased slowly, and charge decreased gradually. Therefore, the change of pH and charge can be caused by proton donation as a function of temperature. Initial and final pH value is not same which is understandable. Because it might take time to go back to the original pH or it is also possible not to gain the same pH again considering the environment.

6.7.b) Direct and Reverse Temperature Variation on Linoleic acid with Pluronic F-127

0.1% Linoleic acid with 5% Pluronic F-127 has been analyzed with direct and reverse temperature cycle to observe the structural property more accurately and to determine if temperature release significantly affect the structure or not. **Figure 43** indicates the change in radius of core, thickness of shell, scattering length density for core and shell, volume fraction and of the particle with respect to temperature.

0.1% Linoleic acid has been coupled with 5% Pluronic F-127 and then measured in SAXS instrument from 10 to 22 ^{0}C with 2 ^{0}C increment and then 22 ^{0}C to 2 ^{0}C with 2 ^{0}C decrement. Analyzed data follow the same pattern for increasing and decreasing temperature and it is a fully reversible cycle. Values of radius, thickness, SLD did not vary significantly with direct and reverse cycle.

a

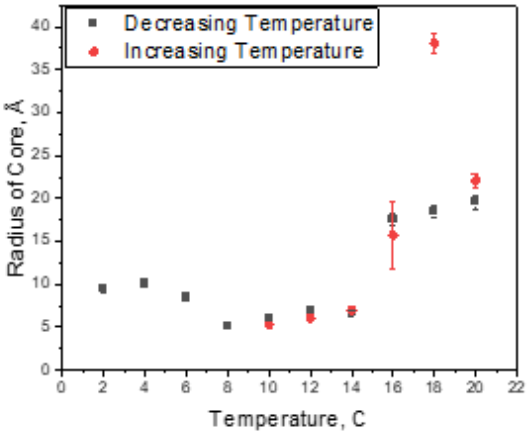

b

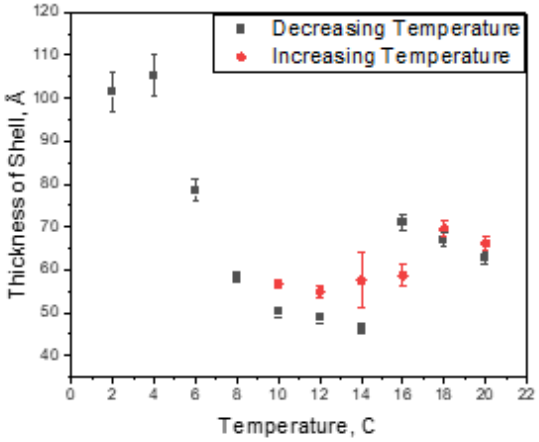

c

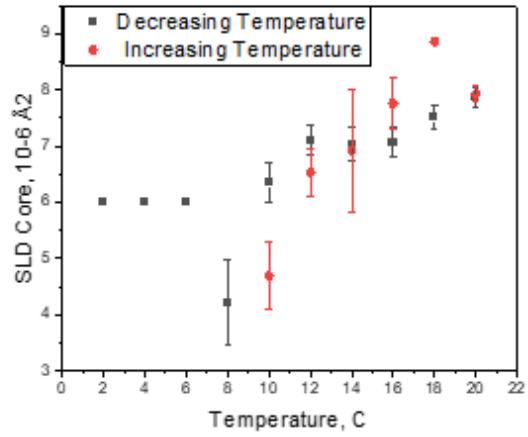

d

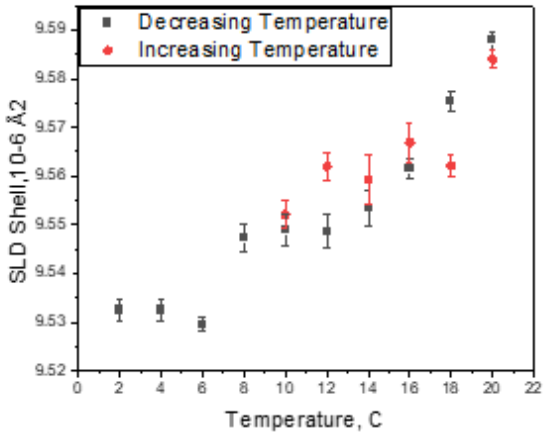

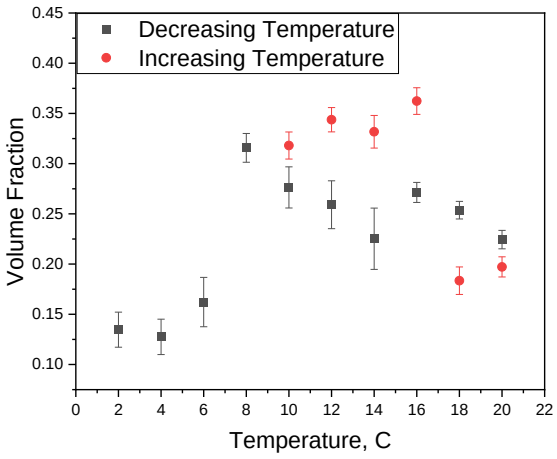

e

Figure 43: Structural properties of 0.1% Linoleic acid with 5% Pluronic F-127 at direct and reverse temperature variation where a) Radius of core b) Thickness of shell c) SLD of core d) SLD of shell e) Volume fraction

The sample experienced transition around 8 ^{0}C-14^{0}C which is visible in radius of core, shell thickness, SLD of core and volume fraction values. Radius increased and thickness decreased at higher temperature. We did not expect a transition at such low temperature, but a transition is clearly visible around 8-14 ^{0}C in all plots of **Figure 43**. As we focused on high temperature dependency of micelles and hydrophobic cargoes because of conventionality of drug delivery, we did not look closely into this matter for this study. But for future study, transition at low temperature deserve a closer look.

7.A)RESULTS FOR PACLITAXEL LOADED PLURONIC F-127

7.1 a) Temperature Dependent Comparison Among Pluronic F-127 Micelles with Paclitaxel, Octane and Linoleic Acid.

In previously measured samples, discrepancy in structural properties have been observed during sample analysis. To estimate the bio accumulations of the samples it is very important to know the distribution ratio of the chemicals which introduces the Octanol-water partition coefficient(logP). logP is ratio of a substance in water-saturated octanol phase and octanol-saturated water phase and it provides useful parameters needed for expressing hydrophilic/lipophilic nature of a substance. If a sample has higher partition coefficient, then solubility and permeability are higher for that composition. For example, Octanol partition coefficient value for Linoleic acid ($C_{18}H_{32}O_2$), Oleic acid ($C_{18}H_{34}O_2$), Octane (C_8H_{18}) are 7.05, 7.64 and 5.15 respectively. [49] Also, Linoleic acid and Oleic acid have pK_a 4.77 and pKa 4.5 respectively. which can be used to get the pH value of the composition.

$$pH = pKa + log_{10}\ \frac{[A-]}{[HA]} \qquad (1)$$

For 0.1% Linoleic acid, pH= 4.77+$\log_{10}$(0.1) =3.77.

Therefore, another batch of samples have been prepared with much lower concentration of alkane, fatty acid and drug. Octane, Linoleic acid and Paclitaxel have been chosen for this measurement and all of the samples have been prepared at low concentration (0.1% Octane+ 5% Pluronic F-127; 0.1% Linoleic acid+ 5% Pluronic F-127; 0.1% Paclitaxel+ 5% Pluronic F-127) at 60 °C. Samples were measured in SAXS at different temperatures (20-60) °C with 5 °C increment.

Micellar pattern has been observed in all samples shown in Figure 4.5.1. The peak increased very slightly for each temperature increment, but structural analysis is needed to get the accurate value of parameters. For 0.1 wt% Paclitaxel with 5 wt% Pluronic F-127, figure showed discrepancy around mid Q value at 60 ^{o}C than other temperature.

a b

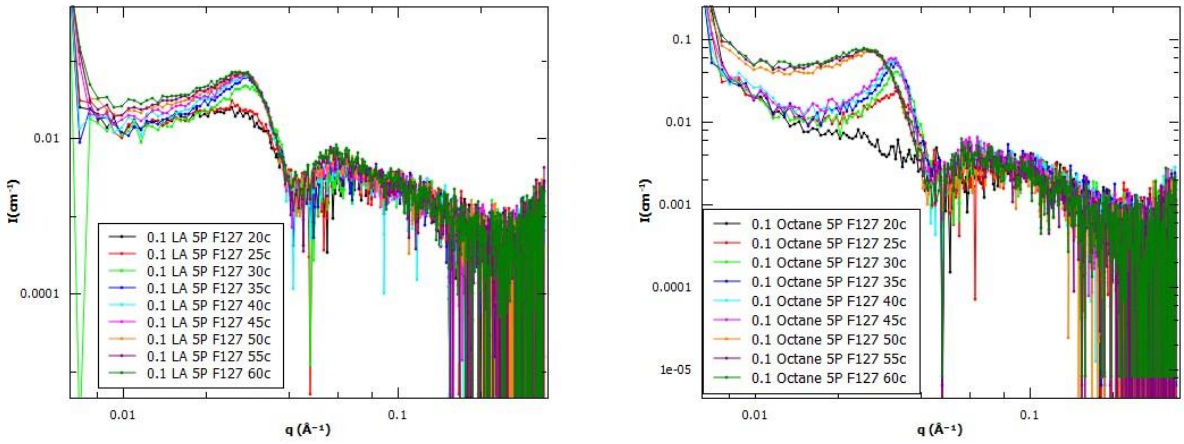

Figure 44: 5% Pluronic F-127 scattering intensity variation with a) 0.1% Linoleic acid and b) 0.1% Octane at different temperature

Figure 44 (a) and (b) shows temperature dependent 0.1% Linoleic acid with 5% Pluronic F-127 and 0.1% Octane with 5% Pluronic F-127 respectively. Error! Reference source not found. shows temperature dependent data of 0.1% Paclitaxel with 5% Pluronic F-127 and only 5% Pluronic F-127.

scattering intensity profile of Paclitaxel indicates the peak shifted toward low q region up to 50 ^{0}C and then shifted right until 60 ^{0}C. That shows gain of inter micellar distance up to 50 ^{0}C and distances between micelles at 55 and 60 ^{0}C. With temperature alteration, Pluronic progresses from dissolved chains to micelles in a fluid like order to micelle crystal structure. All samples reveal sequence of phase changes and signal of fluctuation in composition which implies micellar

formation in the solution. The increase in peak intensity due to phase change also indicates compositional contrast between exterior and interior of micelles and intensity increases rapidly for longer chain length composition than short chain length composition. [38]

It needs to be mentioned that sample at 55-60 ^{0}C have been measured the next day and temperature was increased without any break which might be a possible reason for this discrepancy in scattering profile. Because molecules might not have got enough time to get stabilize for frequent change in temperature.

a b

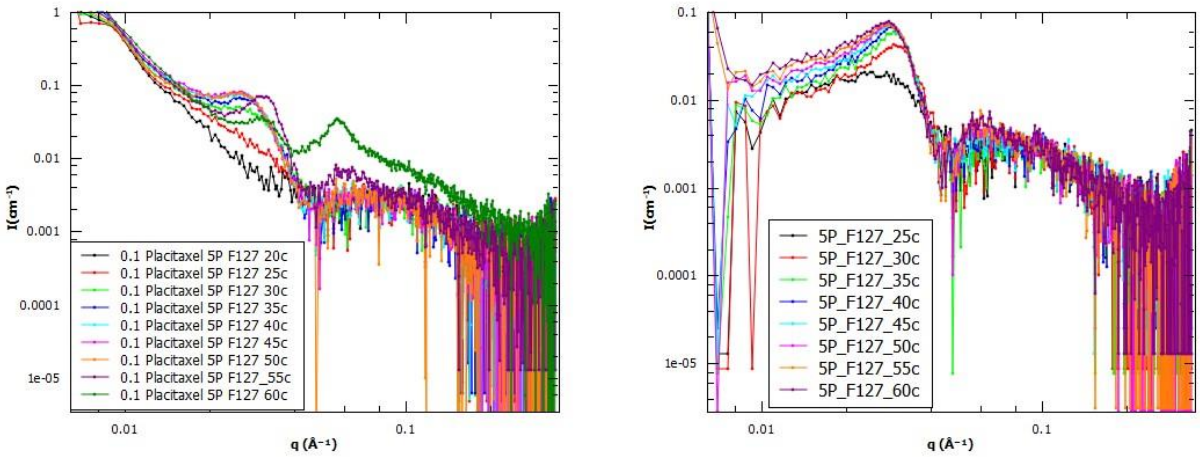

Figure 45: 5% Pluronic F-127 scattering intensity variation with a) 0.1% Paclitaxel and b) Only 5% Pluronic F-127 itself at different temperature

7.b) DISCUSSIONS FOR PACLITAXEL LOADED PLURONIC F-127 MICELLES

7.1. b) Structural Analysis of Paclitaxel with Pluronic F-127 at Different Temperature

Paclitaxel has limited use itself as a treatment for various cancers despite being a chemotherapeutic cytotoxic agent. The main disadvantage of injecting Paclitaxel (PTX) is that it has very poor

solubility, and micelle formulation can help solve this problem. Therefore, Paclitaxel has been loaded with Pluronic F-127 micelles, and several structural properties have been analyzed to get a clearer idea about how these hydrophobic molecules work inside a micelle. 0.1% wt concentration of Paclitaxel has been loaded in 5% Pluronic F-127, and the solution has been mixed with a magnetic hot plate and temperature variant ultrasonic bath. Freshly made F-127 loaded Paclitaxel sample has been measured from 20 ^{0}C to 60 ^{0}C in SAXS instrument for structural analysis. Figure 5.7.1 shows the variation of different parameters with temperature change. A combined Guinier Porod and core-shell hard-sphere model have been applied together on the sample to get the best fit. Calculating the radius of gyration (Rg) can provide information about the particle's mass, shape, and size. A transition in Rg value has been observed in between 35-45 ^{0}C. The core radius stayed unchanged with temperature variation, but the thickness of the shell increased with temperature increment. Whereas temperature variation did not affect the core's scattering length density, the SLD of the shell varied irregularly. The stability of core radius with temperature variation indicates the physical stability of PTX loaded Pluronic F-127 micelles. This also indicates that Pluronic F-127 is a strong candidate for drug encapsulation. Porod exponent is alike for all temperature, but exponent at 35 ^{0}C showed significant error, which might cause improper fitting. The radius of gyration and thickness of the shell is most extensive at 60 ^{0}C, and the radius and SLD of the core are lowest at 60 ^{0}C. 0.1% Paclitaxel with 5% Pluronic F-127 has been compared with the 5% Pluronic F-127 sample in **Figure 46**. Variation in SLD and volume fraction are visible due to Paclitaxel loading. Change of core is not notable after loading Pluronic F-127 with 0.1% Paclitaxel, but a remarkable decrement has been observed in the thickness of the shell.

a

b

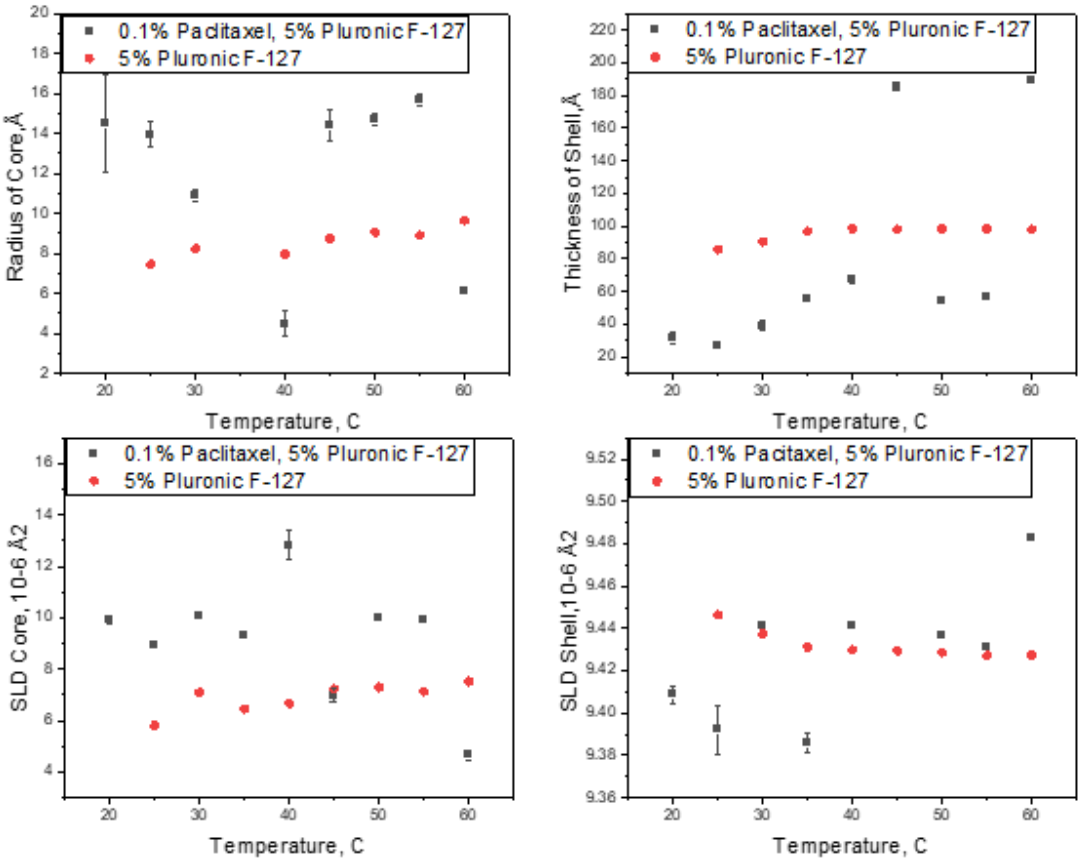

c

d

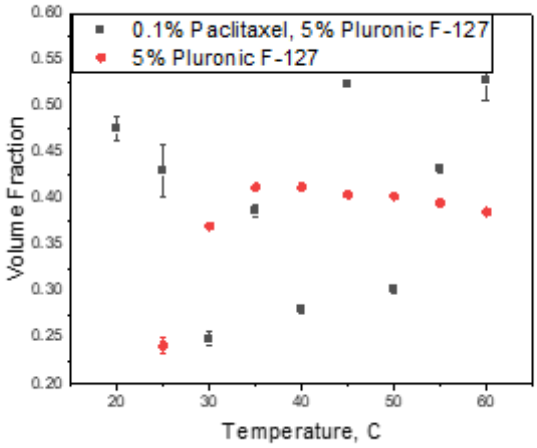

e

Figure 46 Temperature dependent structural parameters of 0.1% Paclitaxel loaded with 5% Pluronic F-127 where a) Radius of core b) Thickness of shell c) SLD core d) SLD shell e) Volume fraction.

Previous studies showed better solubility of PTX in the micellar formulation of surface-active ionic liquid due to hydrogen bonding and cation-π and π-π interactions. According to that study, the micellar formulation can strongly influence the electron density of PTX. [50]

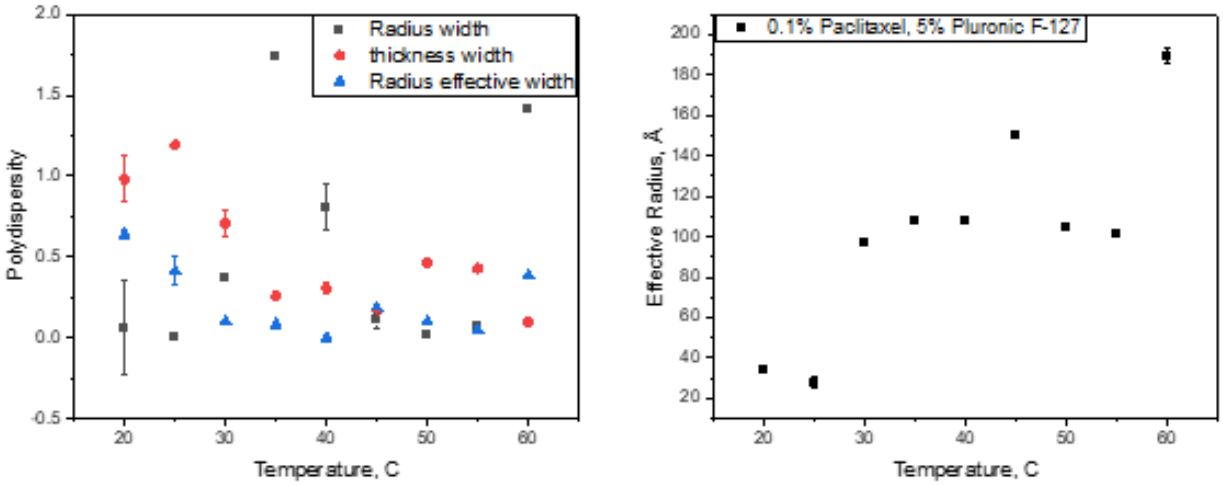

Figure 47 and **Figure 48** conveys, radius of gyration (Rg) is three times more than the effective radius. This means Rg value is almost equal to 2-3 micelle clusters. As Paclitaxel is a large molecule, 5% Pluronic F-127 might be too small concentration to encapsulate it. Because of it's larger volume, it is difficult to relate the scattering length density value as well.

At high temperatures, PPO blocks of Pluronic F-127 become more hydrophobic, and the core contains less water, and PEO dissolves in micellar corona, which contains a large amount of water. Hammouda et al. studied that not all surfactant molecules convert into micelle as some of them homogenously dissolve in the solvent, and the fraction of SDS (Sodium dodecyl sulfate) surfactant in the micelles decreased with temperature. This might be due to micellar formation softening. [42] Acknowledging this finding, we can predict that the dissolved surfactants at a high temperature can be a reason for having irregular volume fractions. This irregular structural variation indicates significant inter-micelle interaction, which might be a barrier for systematic variation with temperature. Among all the materials used in this study, Paclitaxel is the only

molecule that is not liquid at room temperature. Therefore, to encapsulate it inside the micelle, it must be dissolved in another solvent earlier. So, the next logical step is to dissolve Paclitaxel in a non-polar solvent such as Oleic acid or Linoleic acid before loading with Pluronic F-127 micelles. A lower concentration of Paclitaxel, a more significant concentration of Pluronic F-127, and the addition of another hydrophobic molecule to dissolve Paclitaxel could be practical steps to take in the future.

a b

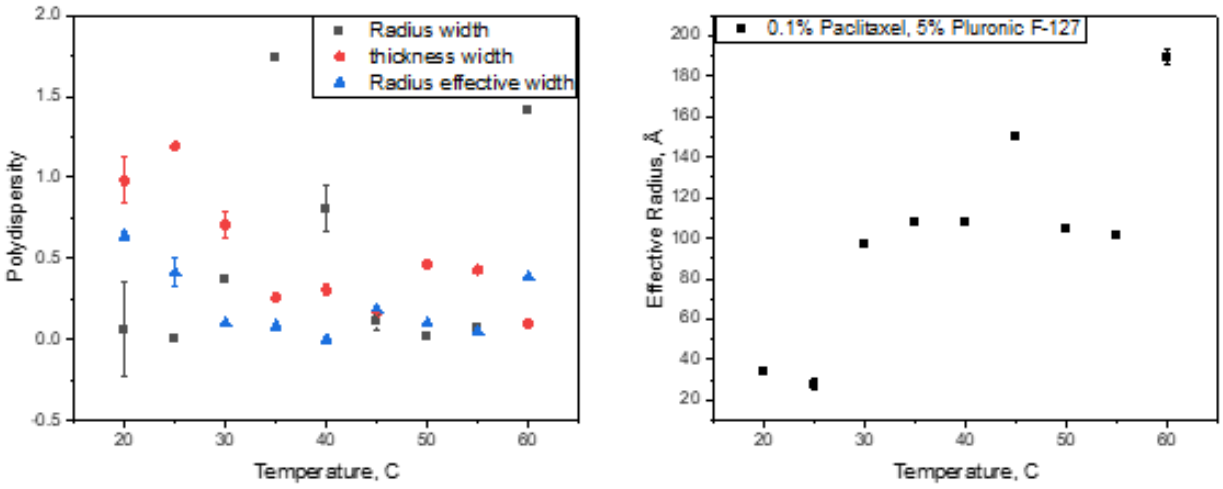

Figure 47 Temperature dependent structural parameters of 0.1% Paclitaxel loaded with 5% Pluronic F-127 where a) Polydispersity b) Effective radius.

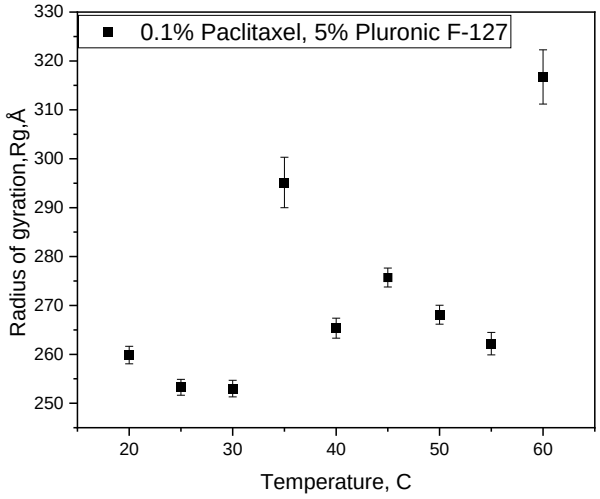

Figure 48 Radius of gyration with temperature variation for 0.1% Paclitaxel with 5% Pluronic F-127.

8. CONCLUSION

A scattering intensity profile as a scattering vector has been studied for Pluronic F-127 with different weight concentrations. Radius and SLD of core increased, volume fraction, thickness, and SLD shell decreased in 5% Pluronic F-127 samples. Micelle formation is affected by temperature and concentration depending on cargoes and visible around 20-30 ^{0}C. Also, the sol-gel transition has been observed around 35-40 ^{0}C. 5% Pluronic F-127 loaded with 5% alkanes (Hexane, Octane, Decane, and Dodecane) prepared at room temperature indicates an increase in core radius and decrease in shell thickness with increasing alkane number conveying the increased size of the hydrophobic core with alkanes with a longer chain. Analysis of Pluronic F-127 with alkanes (Decane, Dodecane) at different concentrations 1%,5%, 10% prepared at 60 ^{0}C shows an increase of core radius and decrease of shell thickness with increasing weight concentration. The scattering intensity profiles of Linoleic and Oleic acid are different from different sample filled Kapton tube positions. In contrast, scattering intensity is identical for Pluronic F-127 micelles, which shows the homogeneity of Pluronic samples, but the non-uniform solution of fatty acid loaded Pluronic F-127. 1% and 5% Oleic acid along with 2.5% Pluronic F-127 and 2% and 10% Oleic acid with 5% Pluronic F-127 showed comparable structural properties for 1% and 2% Oleic acid, which is expected as both samples have the same ratio of components. However, 10% Oleic acid and 10% Dodecane samples did not let the micelle form because of having too much concentration. The possibility of less concentration of Oleic acid presence arises due to higher concentration and increasing thickness of the shell. The micellar formation is clear from the scattering spectrum of low concentration Linoleic acid (0.05%, 0.1%, 0.2%) and in temperature-dependent Pluronic F-127 with and without Linoleic acid, Octane, and Paclitaxel. This is a sign that temperature and concentration play a crucial role in micelle formation. Micelle formation and

sol-gel transition have been observed during sample analysis through core-shell modeling. The pH value also decreased with increasing Linoleic acid concentration and pH cycle, increasing and decreasing temperature followed by a pattern. Direct and reverse temperature variation of Pluronic F-127 and Linoleic acid loaded Pluronic F-127 did not show any significant variation, which confirms that samples are affected by temperature and fully reversible. Finally, the Paclitaxel data showed irregular value because of having a way larger molecule than Pluronic F-127. The addition of another hydrophobic molecule is needed for dissolving Paclitaxel in the solution.

REFERENCES

[1] G. Tiwari *et al.*, "Drug delivery systems: An updated review," *Int. J. Pharm. Investig.*, vol. 2, no. 1, p. 2, 2012, doi: 10.4103/2230-973x.96920.

[2] H. A. E. Benson and A. C. Watkinson, *Topical and Transdermal Drug Delivery*. Hoboken, NJ, USA: John Wiley & Sons, Inc., 2011.

[3] W. Xu, P. Ling, and T. Zhang, "Polymeric Micelles, a Promising Drug Delivery System to Enhance Bioavailability of Poorly Water-Soluble Drugs," *J. Drug Deliv.*, vol. 2013, pp. 1–15, Jun. 2013, doi: 10.1155/2013/340315.

[4] S. Chatterjee, P. C. leung Hui, C. wai Kan, and W. Wang, "Dual-responsive (pH/temperature) Pluronic F-127 hydrogel drug delivery system for textile-based transdermal therapy," *Sci. Rep.*, 2019, doi: 10.1038/s41598-019-48254-6.

[5] R. Basak and R. Bandyopadhyay, "Encapsulation of Hydrophobic Drugs in Pluronic F127 Micelles: Effects of Drug Hydrophobicity, Solution Temperature, and pH," 2013, doi: 10.1021/la304836e.

[6] E. Giuliano, D. Paolino, M. Fresta, and D. Cosco, "Mucosal applications of poloxamer 407-based hydrogels: An overview," *Pharmaceutics*, vol. 10, no. 3. MDPI AG, p. 159, Sep. 12, 2018, doi: 10.3390/pharmaceutics10030159.

[7] A. M. Bodratti and P. Alexandridis, "Formulation of poloxamers for drug delivery," *Journal of Functional Biomaterials*, vol. 9, no. 1. MDPI AG, p. 11, Jan. 18, 2018, doi: 10.3390/jfb9010011.

[8] S. Kerkhofs *et al.*, "Self-Assembly of Pluronic F127 - Silica Spherical Core-Shell Nanoparticles in Cubic Close-Packed Structures," *Chem. Mater.*, vol. 27, no. 15, pp. 5161–5169, Aug. 2015, doi: 10.1021/acs.chemmater.5b01772.

[9] M. Callan *et al.*, "Characterization of Pluronic F 127 for the Controlled Drug Release Vancomycin in the Spinal Column," 2017.

[10] Q. Gao, Q. Liang, F. Yu, J. Xu, Q. Zhao, and B. Sun, "Synthesis and characterization of novel amphiphilic copolymer stearic acid-coupled F127 nanoparticles for nano-technology based drug delivery system," *Colloids Surfaces B Biointerfaces*, vol. 88, no. 2, pp. 741–748, Dec. 2011, doi: 10.1016/j.colsurfb.2011.08.010.

[11] J. C. Gilbert, J. Hadgraft, A. Bye, and L. G. Brookes, "Drug release from Pluronic F-127 gels," *Int. J. Pharm.*, vol. 32, no. 2–3, pp. 223–228, Oct. 1986, doi: 10.1016/0378-5173(86)90182-1.

[12] "Hydrophobic Interactions - Chemistry LibreTexts." https://chem.libretexts.org/Bookshelves/Physical_and_Theoretical_Chemistry_Textbook_Maps/Supplemental_Modules_(Physical_and_Theoretical_Chemistry)/Physical_Properties_of_Matter/Atomic_and_Molecular_Properties/Intermolecular_Forces/Hydrophobic_Interactions (accessed Jan. 27, 2021).

[13] H. Zhong *et al.*, "Aggregate-based sub-CMC solubilization of n-alkanes by

monorhamnolipid biosurfactant," *New J. Chem.*, vol. 40, no. 3, pp. 2028–2035, 2016, doi: 10.1039/c5nj02108a.

[14] R. Kumar, A. Sirvi, S. Kaur, S. K. Samal, S. Roy, and A. T. Sangamwar, "Polymeric micelles based on amphiphilic oleic acid modified carboxymethyl chitosan for oral drug delivery of bcs class iv compound: Intestinal permeability and pharmacokinetic evaluation," *Eur. J. Pharm. Sci.*, vol. 153, p. 105466, Oct. 2020, doi: 10.1016/j.ejps.2020.105466.

[15] "Oleic acid | C18H34O2 - PubChem." https://pubchem.ncbi.nlm.nih.gov/compound/445639 (accessed May 08, 2021).

[16] "Linoleic acid | C18H32O2 - PubChem." https://pubchem.ncbi.nlm.nih.gov/compound/Linoleic-acid (accessed May 08, 2021).

[17] "Fatty Acids -- Classification of Fatty Acids." https://library.med.utah.edu/NetBiochem/FattyAcids/3_3.html (accessed May 08, 2021).

[18] "Paclitaxel | C47H51NO14 - PubChem." https://pubchem.ncbi.nlm.nih.gov/compound/taxol#section=LC-MS (accessed May 11, 2021).

[19] M. Rezazadeh, V. Akbari, E. Amuaghae, and J. Emami, "Preparation and characterization of an injectable thermosensitive hydrogel for simultaneous delivery of paclitaxel and doxorubicin," *Res. Pharm. Sci.*, vol. 13, no. 3, pp. 181–191, Jun. 2018, doi: 10.4103/1735-5362.228918.

[20] "Surfactants & critical micelle concentration (CMC) - DataPhysics Instruments." https://www.dataphysics-instruments.com/us/knowledge/understanding-interfaces/surfactants-cmc/ (accessed May 09, 2021).

[21] Y. Lin and P. Alexandridis, "Temperature-Dependent Adsorption of Pluronic F127 Block Copolymers onto Carbon Black Particles Dispersed in Aqueous Media," 2002, doi: 10.1021/jp014221i.

[22] J. Lipfert and S. Doniach, "Small-Angle X-Ray Scattering from RNA, Proteins, and Protein Complexes," *Annu. Rev. Biophys. Biomol. Struct.*, vol. 36, no. 1, pp. 307–327, Jun. 2007, doi: 10.1146/annurev.biophys.36.040306.132655.

[23] "Conduction of electricity through gases | HathiTrust Digital Library." https://catalog.hathitrust.org/Record/001482204 (accessed Jan. 28, 2021).

[24] J. I. Goldstein *et al.*, "Electron Beam—Specimen Interactions: Interaction Volume," in *Scanning Electron Microscopy and X-Ray Microanalysis*, Springer New York, 2018, pp. 1–14.

[25] A. Agbabiaka, M. Wiltfong, and C. Park, "Small Angle X-Ray Scattering Technique for the Particle Size Distribution of Nonporous Nanoparticles," *J. Nanoparticles*, vol. 2013, pp. 1–11, Dec. 2013, doi: 10.1155/2013/640436.

[26] "(8) (PDF) Small Angle X-ray Scattering of Group V Polyoxometalates." https://www.researchgate.net/publication/279192449_Small_Angle_X-

ray_Scattering_of_Group_V_Polyoxometalates (accessed Apr. 27, 2021).

[27] "New generation X-ray beam delivery system - Xenocs." https://www.xenocs.com/new-generation-x-ray-beam-delivery-system/ (accessed Apr. 27, 2021).

[28] "Bragg's Law - Sciencetopia." https://www.sciencetopia.net/physics/braggs-law (accessed Apr. 28, 2021).

[29] "PILATUS3 R 200K-A - Dectris." https://www.dectris.com/products/pilatus3/pilatus3-r-for-laboratory/pilatus3-r-200k-a/ (accessed Apr. 28, 2021).

[30] "The SAXS Guide. Getting acquainted with the principles - PDF Free Download." https://docplayer.net/51986599-The-saxs-guide-getting-acquainted-with-the-principles.html (accessed Apr. 28, 2021).

[31] "fractal_core_shell — SasView 5.0.4 documentation." http://www.sasview.org/docs/user/models/fractal_core_shell.html (accessed May 11, 2021).

[32] "hardsphere — SasView 5.0.4 documentation." https://www.sasview.org/docs/user/models/hardsphere.html (accessed May 11, 2021).

[33] "hayter_msa — SasView 5.0.4 documentation." http://www.sasview.org/docs/user/models/hayter_msa.html (accessed May 11, 2021).

[34] "guinier_porod — SasView 5.0.4 documentation." https://www.sasview.org/docs/user/models/guinier_porod.html (accessed May 11, 2021).

[35] Y. Li, T. Shi, Z. Sun, L. An, and Q. Huang, "Investigation of Sol-Gel Transition in Pluronic F127/D 2 O Solutions Using a Combination of Small-Angle Neutron Scattering and Monte Carlo Simulation," 2006, doi: 10.1021/jp066019r.

[36] K. Mortensen, W. Brown, and B. Nordén, "Inverse melting transition and evidence of three-dimensional cubatic structure in a block-copolymer micellar system," *Phys. Rev. Lett.*, vol. 68, no. 15, pp. 2340–2343, 1992, doi: 10.1103/PhysRevLett.68.2340.

[37] C. Wu, T. Liu, B. Chu, D. K. Schneider, and V. Graziano, "Characterization of the PEO-PPO-PEO triblock copolymer and its application as a separation medium in capillary electrophoresis," *Macromolecules*, vol. 30, no. 16, pp. 4574–4583, Aug. 1997, doi: 10.1021/ma9701088.

[38] H. Yardimci, B. Chung, J. L. Harden, and R. L. Leheny, "Phase behavior and local dynamics of concentrated triblock copolymer micelles," *J. Chem. Phys.*, vol. 123, no. 24, p. 244908, Dec. 2005, doi: 10.1063/1.2132278.

[39] L. M. Bergström, "A theoretical investigation of the influence of the second critical micelle concentration on the solubilization capacity of surfactant micelles," *AIP Adv.*, vol. 8, no. 5, May 2018, doi: 10.1063/1.5027062.

[40] H. Hoffmann and W. Ulbricht, "Transition of rodlike to globular micelles by the solubilization of additives," *J. Colloid Interface Sci.*, vol. 129, no. 2, pp. 388–405, May 1989, doi: 10.1016/0021-9797(89)90453-0.

[41] Y.-T. Wu, J.-L. Chai, X.-Q. Li, B. Yang, S.-C. Shang, and J.-J. Lu, “Effect of Alkane/Water Ratios on the Phase Behavior and the Solubilization of Microemulsion Systems Containing Hexadecyltrimethylammonium Bromide,” *J. Chem. Eng. Data*, vol. 56, pp. 3089–3094, 2011, doi: 10.1021/je2000793.

[42] B. Hammouda, “Temperature Effect on the Nanostructureof SDS Micelles in Water,” *J. Res. Natl. Inst. Stand. Technol.*, vol. 118, p. 151, Apr. 2013, doi: 10.6028/jres.118.008.

[43] D. G. Isom, C. A. Castañeda, B. R. Cannon, P. D. Velu, and B. García-Moreno E, “Charges in the hydrophobic interior of proteins,” *Proc. Natl. Acad. Sci. U. S. A.*, vol. 107, no. 37, pp. 16096–16100, Sep. 2010, doi: 10.1073/pnas.1004213107.

[44] H. P. Lehmann, X. Fuentes-Arderiu, and L. F. Bertello, “Glossary of terms in quantities and units in clinical chemistry (IUPAC-IFCC recommendations 1996),” *Pure Appl. Chem.*, vol. 68, no. 4, pp. 957–1000, Jan. 1996, doi: 10.1351/pac199668040957.

[45] O. Yuki, Y. Zhang, J. Ge, and Z. Liu, “Epoxidation of Fatty Acids by Pluronic-Conjugated Lipase in Organic Media,” *Catal. Letters*, vol. 146, no. 6, pp. 1073–1078, Jun. 2016, doi: 10.1007/s10562-016-1726-5.

[46] D. D. Guo *et al.*, “Enhanced anticancer effect of conjugated linoleic acid by conjugation with Pluronic F127 on MCF-7 breast cancer cells,” *Cancer Lett.*, vol. 254, no. 2, pp. 244–254, Sep. 2007, doi: 10.1016/j.canlet.2007.03.007.

[47] V. Escuyers9, P. Boquet$, D. Perrint, C. Montecuccoii, and M. Mock, “A pH-induced increase in hydrophobicity as a possible step in the penetration of colicin E3 through bacterial membranes.,” 1986. doi: 10.1016/S0021-9258(18)67471-X.

[48] C. B. Castells, C. Ràfols, M. Rosés, and E. Bosch, “Effect of temperature on pH measurements and acid-base equilibria in methanol-water mixtures,” *J. Chromatogr. A*, vol. 1002, no. 1–2, pp. 41–53, Jun. 2003, doi: 10.1016/S0021-9673(03)00644-7.

[49] J. Sangster, “Octanol Water Partition Coefficients of Simple Organic Compounds,” *J. Phys. Chem. Ref. Data*, vol. 18, no. 3, pp. 1111–1229, Jul. 1989, doi: 10.1063/1.555833.

[50] M. K. Ali, R. M. Moshikur, R. Wakabayashi, M. Moniruzzaman, and M. Goto, “Biocompatible Ionic Liquid-Mediated Micelles for Enhanced Transdermal Delivery of Paclitaxel,” *ACS Appl. Mater. Interfaces*, p. acsami.1c03111, Apr. 2021, doi: 10.1021/acsami.1c03111.

APPENDIX

Appendix A: Process of Data Reduction by Foxtrot

The following steps are used to reduce data from Foxtrot:

- Open Foxtrot icon and go to files to load required ".edf " files on foxtrot.

- To find direct beam integrated values

  Select direct beam '.edf' file ≫ click rectangular ROI mode and make a rectangle around the centre ≫ go to operation and perform integral.

- To find the transmission coefficient, copy all the direct beam integrated values and create a table in a spreadsheet. Transmission coefficient is then obtained by dividing the integrated value sample or buffer with the integrated values of empty instrument.

- To convert 2D raw data to 1D raw data:

  Select raw '.edf' files ≫ load a mask (if you don't have a mask make mask first) ≫ go to operation and perform circle gathering ≫ go to operation toolbar and click the second last icon to export all the circular averaged raw '.edf' to '.dat' and save it.

Appendix B: Process of Data Reduction by Mantidplot

The following procedure is used to reduce data using MantidPlot:

- Create folders for raw '.edf' files produced by the instrument, circular averaged '.dat' files from Foxtrot, reductionScripts and MantidPlot results

- Open Mantidplot icon and load python script as follow:

- Go to Files ≫ Manage user directories ≫ select python script directory ≫ Enter or browse to the location of the Xeuss '.py' script files ≫ click Ok

This process needs to be done just once, unless you change the location of your scripts.

- To initiate processing Xeuss data:

Go to view ≫ Script window (this will open a new script window) ≫ in the new script window go to files ≫ open ≫ choose the required '.py' files.

- To execute commands within a script:

Select command ≫ go to Execute ≫ Execute Selection (for shortcut: CTRL+ Enter, to execute all CTRL+Shift+Enter)

There are many available Xeuss functions like XeussLoadLogger, XeussLoad, XeussReduce and so on. Each have its own function.

VITA

Tahmida Raheen Iqbal completed her undergraduate and graduate studies in Physics from University of Dhaka in Bangladesh. She came to University of Texas at El Paso (UTEP) for her master's degree in Physics in 2019. She availed one time award "C. Sharp Cook Graduate Fellowship Fund in 2019-2020 academic year. Her research has been presented in conferences such as American Physical Society (APS) March meeting and COURI summer symposium.

In Bangladesh she worked as a research scientist at Bangladesh Atomic Energy Commission for one year. In her current University (UTEP), she worked as a Teaching Assistant for two years. Her research during this period was focused on biophysics, particularly studying the structural variation in micelles loaded with different hydrophobic cargoes. Now, with an MS in Physics she will be joining Georgetown University for her doctoral study from the Fall 2021.